Interleukin 6 drives durable T cell-mediated immunity to pancreatic cancer

Short title: IL-6 drives durable T cell immunity in PDAC

Paige C. Arneson-Wissink[1], Alexandra Q. Bartlett[2], Heike Mendez[1], Xinxia Zhu[1], Jessica Dickie[1], Matthew McWhorter[2], Peter R. Levasseur[1], Parham Diba[1], Katelyn T. Byrne[3,4], Gregory D. Scott[5], Robert Eil[2], Aaron J. Grossberg[1, 4, 6]*

[1] Department of Radiation Medicine, Oregon Health & Science University, Portland, OR, 97239, USA

[2] Division of Surgical Oncology, Department of Surgery, Knight Cancer Institute, Oregon Health & Science University, Portland, OR, 97239, USA

[3] Department of Cell, Development, and Cancer Biology, Oregon Health & Science University, Portland, OR, 97239, USA

[4] Brenden Colson Center for Pancreatic Care, Oregon Health & Science University, Portland, OR, 97239, USA

[5] Department of Pathology, Oregon Health & Science University, Portland, OR, 97239, USA

[6] Cancer Early Detection Advanced Research Center, Oregon Health & Science University, Portland, OR, 97201, USA

***Corresponding Author**: Aaron J. Grossberg, 3181 SW Sam Jackson Park Rd Mail Code L481, Oregon Health and Science University, Portland, OR, 97239, 503-494-9945, grossber@ohsu.edu

Preprint Server: https://doi.org/10.1101/2024.09.26.615308

Word Count: 2788

Grant Support: This work was supported by the National Cancer Institute (PCAW: K99CA286709; AJG: K08CA245188, R37CA280692, R01CA264133; RE: K08CA256179), the Brenden Colson Center for Pancreatic Care, the Oregon Pancreas Tissue Registry, the Histopathology Shared Resource for pathology studies (University Shared Resource Program at Oregon Health and Sciences University and the Knight Cancer Institute (P30 CA069533 and P30 CA069533 13S5)), the OHSU Flow Cytometry Shared Resource (OHSU Knight Cancer Institute NCI Cancer Center Support Grant P30CA069533), and the Advanced Multiscale Microscopy Shared Resource (OHSU Knight Cancer Institute, NIH P30 CA069533). RE was also supported by grants from the American Association of Cancer Research, ASCO, and Pancreatic Cancer Action Network.

Data Transparency: All data will be available on the public repository, Mendeley Data, upon publication. Further information and resources, including plasmid sequences, engineered KPC cells, and raw data will be shared upon reasonable request to Aaron J. Grossberg (grossber@ohsu.edu).

Disclosures: RE is a paid consultant and conducts ongoing research for Lyell Immunopharma. KTB receives consultation feed from Guidepoint Global and royalties from the University of Pennsylvania for licensed research cell lines. The other authors declare no conflicts.

Abbreviations:

BSR	Blasticidin Resistance

CAR	Chimeric Antigen Receptor
CD	Cell Differentiation
ELISA	Enzyme-Linked Immunosorbent Assay
Fbxo32	F-Box Protein 32
Foxp3	Forkhead Box Protein P3
H&E	Hematoxylin and Eosin
IL-6	Interleukin 6
KPC	$Kras^{G12D/+}$, $Tp53^{R172H/+,}$ Pdx1-Cre
NK	Natural Killer
OT-PDAC	Orthotopic Pancreatic Ductal Adenocarcinoma
PDAC	Pancreatic Ductal Adenocarcinoma
Qpcr	Quantitative Polymerase Chain Reaction
Trim63	Tripartite Motif Containing 63

SYNOPSIS

Interleukin-6 induces rapid and durable T cell-driven immune clearance of pancreatic ductal adenocarcinoma. The anti-tumor immune microenvironment is hallmarked by increased lymphoid aggregate formation, increased CD4 T cell abundance, and decreased Treg abundance.

ABSTRACT

Background & Aims: Tumor immune resistance is recognized as a contributor to low survivorship in pancreatic ductal adenocarcinoma (PDAC). The inflammatory cytokine interleukin-6 (IL-6) promotes polarization of CD4 T cell populations away from immune tolerance, induces differentiation of cytotoxic CD8 T cells, and drives expansion and anti-tumor activity in chimeric antigen receptor (CAR) T cell therapies. This work aims to test whether IL-6 could stimulate an anti-tumor response in PDAC

Methods: We overexpressed IL-6 in multiple $Kras^{G12D/+}$, $Tp53^{R172H/+,}$ Pdx1-Cre (KPC) cell lines, which were orthotopically implanted in mice ($OT\text{-}PDAC^{IL6}$). We followed mouse survival and measured tumor growth, tumor histology, and plasma IL-6 at 5 and 10 days after tumor implantation. We measured tumor immune cell infiltration via flow cytometry and histology. We used antibody-based T cell depletion and secondary tumor implantation rechallenge to test the dependency of the durable immune reaction on T cells.

Results: Improved survival occurred in all instances of $OT\text{-}PDAC^{IL6}$, with one cell line (KxPxCx) reproducibly resulting in long-term recurrence-free survival. With KxPxCx cells,

circulating IL-6 was 100-fold higher in OT-PDAC^{IL6} than in OT-PDAC^{parental} mice. Flow cytometry revealed increased T cells and NK cells, and decreased T regulatory cells, and we observed significantly increased lymphoid aggregates in OT-PDAC^{IL6} as compared to OT-PDAC^{parental} tumors. Antibody-based CD4^{+} and CD8^{+} T cell depletion prevented tumor clearance and completely abolished the survival advantage in OT-PDAC^{IL6} mice. The anti-tumor immune response to OT-PDAC^{IL6} rendered mice immune to re-challenge with OT-PDAC^{parental} tumors.

Conclusions: Locally high IL-6 concentrations potently enhance the T cell-mediated anti-tumor response to PDAC.

Key words: Interleukin 6; Pancreatic Ductal Adenocarcinoma; T regulatory cells

INTRODUCTION

Pancreatic ductal adenocarcinoma (PDAC) is associated with an immunosuppressive microenvironment, characterized by low numbers of infiltrating T cells and relatively higher numbers of immunosuppressive T regulatory cells (Tregs)[1, 2]. Despite clinical trials that have established the safety of immunotherapies in PDAC, the immune profile of PDAC limits the clinical efficacy of these interventions[3]. Conversely, increased T cell infiltration with low Treg infiltration is associated with improved patient survival [5]. Strategies that promote T cell activation, such as agonizing CD40 antibodies, increase tertiary immune structure formation and benefit mouse survival in pre-clinical models[4]. A small but growing body of literature suggests that tumor-localized expression of immunomodulatory cytokines, such as IL-6, IL-12, CXCL13, and CCL21 can also improve immune reactivity to tumors by driving localization and differentiation of tumor-infiltrating lymphocytes, which accumulate in tertiary lymphoid structures or lymphoid aggregates[5-7].

Interleukin-6 (IL-6) signaling is associated with reduced survival in patients with PDAC attributed to the promotion of tumorigenesis and metastasis [8-11]. Elevated circulating IL-6 also associates with sarcopenia in PDAC patients, and we previously demonstrated that host intrinsic IL-6 signaling is necessary for mice to develop PDAC cachexia[12]. Published literature shows that loss of IL-6 attenuates PDAC development, metastasis, and cachexia onset [12-14]. However, IL-6 is also well-established as an immunomodulatory cytokine and contributes to polarization of CD4 T cell populations, differentiation of cytotoxic CD8 T cells, inhibition of inducible Treg development, and expansion and anti-tumor activity in chimeric antigen receptor (CAR) T cell therapies[15-17]. Leveraging the immunomodulatory properties of IL-6 may promote

anti-tumor immunity in PDAC.

In the current study, we sought to investigate the effect of IL-6 overexpression on immune clearance of PDAC and cachexia development. We developed stable IL-6 overexpressing PDAC cells ($PDAC^{IL6}$) from $PDAC^{parental}$ (KPC) cell lines[18]. We found that $PDAC^{IL6}$ cells produced extremely high levels of IL-6 and induced severe cachexia within days of orthotopic implantation (OT-$PDAC^{IL6}$). We also observed dramatic changes in tumor growth dynamics, with one cell line eliciting complete tumor clearance and long-term, recurrence-free mouse survival. We then pursued a series of studies to understand the immune response to high intra-tumoral IL-6. The work shown here presents IL-6 overexpression as a driver of T cell infiltration in PDAC, which poises mice for a favorable anti-tumor immune response.

RESULTS

Tumor-specific IL-6 overexpression induces spontaneous tumor clearance and cachexia recovery. We developed $PDAC^{IL6}$ cells from the KPC PDAC cell line KxPxCx, using ecotropic retroviral transduction. We first observed that mice implanted with OT-$PDAC^{IL6}$ tumors experienced nearly 100% survival without reaching terminal endpoints (**Figure 1A**). OT-$PDAC^{IL6}$ mice euthanized approximately 10 days after all OT-$PDAC^{parental}$ had significantly lower tumor/pancreas mass, and no detectable IL-6 in the plasma (**Figure 1B-C**). Deeper histological assessment of tumors showed that both OT-$PDAC^{IL6}$ and OT-$PDAC^{parental}$ developed poorly differentiated, infiltrative carcinoma by five days (**Figure 1D-F**). OT-$PDAC^{IL6}$ tumors were slightly smaller in mass and histological area than OT-$PDAC^{parental}$ tumors (**Figure 1F-G**). By 12 days, OT-$PDAC^{parental}$ mice had reached humane euthanasia endpoint, with

carcinoma covering approximately 80% of total tissue area, in contrast, OT-PDAC^{IL6} tissue was completely devoid of tumor (**Figure 1E,G, Table S1**). We confirmed this result molecularly using qPCR for the codon-optimized *Il6* transgene, which was not detected in OT-PDAC^{IL6} whole pancreas tissue after five days (**Figure 1H, Figure S1**). While lung and liver metastases were detected by *Il6* transgene qPCR at five days, there were no metastases detected at 12 days (**Figure S2**). Spontaneous tumor clearance also occurred when PDAC^{IL6} cells were implanted subcutaneously, indicating that the phenomenon is not specific to intrapancreatic administration (**Figure S3**).

OT-PDAC^{parental} plasma IL-6 levels were in line with previously published values, while OT-PDAC^{IL6} levels reached 100-fold higher levels at day 5, followed by undetectable levels at later time points (**Figure 1I**) [10, 12]. Because high circulating IL-6 is associated with cachexia development in PDAC, we investigated total body and muscle mass[10]. High plasma IL-6 and peak tumor burden associated with decreased body mass, which recovered with the normalization of IL-6 levels after tumor clearance in the OT-PDAC^{IL6} model (**Figure 1J**). Gross muscle mass trended downward at five days and was significantly decreased at 10 days, while muscle atrophy gene (*Trim63* and *Fbxo32*) expression was elevated at 5 days and reduced to baseline at 10 days. These data reflect a delay in tissue recovery as the tumor resolves and body mass returns to baseline (**Figure 2K-L**). Collectively, these data show that IL-6 overexpression in PDAC cells leads to severe wasting, followed by body mass recovery upon spontaneous tumor resolution.

Multiple OT-PDAC^{IL6} cell lines, but not CD90.1 transduction control lines, display improved survival outcomes. We then tested whether the impact of IL-6 overexpression on

tumor clearance and mouse survival applied to other murine PDAC cell lines: KPC-1199[19], and KPC-1242[20]. While both PDAC^{IL6} cell lines had significantly improved survival, only OT-1242^{IL6} dissected tumor masses at humane endpoint showed a significant reduction, when compared to the respective parental control line (**Figure 2A-B, D-E**). Plasma IL-6 levels at endpoint reflected tumor burden: 1242^{IL6} caused ~250 fold elevation of IL-6, and 1199^{IL6} did not show a significant change (**Figure 2C,F**). We validated the clearance and survival phenotypes using an independently generated KxPxCx^{IL6} (KX2^{IL6}) (**Figure 2G-I**). This lead us to hypothesize that reduced tumor mass correlated specifically with IL-6 overexpression. We tested this by using a KxPxCx transduction control cell line, where we expressed CD90.1 alone without IL-6 (OT-PDAC$^{CD90.1)}$. OT-PDAC$^{CD90.1}$ mice replicated our findings with non-transduced OT-PDAC^{parental} mice. Both groups had reached humane euthanasia endpoint by 12 days, carcinoma covering approximately 80% of total tissue area, circulating IL-6 elevated to the expected 200-300 pg/mL range, and body mass loss not exceeding 10% (**Figure 2J-M, Table S1**). Finally, we tested the tumor response to IL-6 overexpression when fewer cells are implanted, thus prolonging the period of host exposure to tumor before humane euthanasia criteria are met. We tested 5,000 KxPxCx cells, 100,000 KPC-1199 cells, and 100,00 KPC-1242 cells, and found that survival, tumor mass, and plasma IL-6 replicated our findings with 1 million cell implantation doses (**Figure 3A-I**). We therefore concluded that the tumor clearance we observed was specific to IL-6 overexpression and most robust in the KxPxCx cell line, which we selected for continued testing. Because we did not observe a dose-dependent effect, we proceeded to exclusively test the implantation dose of 1 million KxPxCx^{IL6} cells, which aligns with our previously published work (from here on, termed OT-PDAC^{IL6}).[12]

OT-PDAC^{IL6} induces lymphocytic anti-tumor immune response. Spleens from OT-PDAC^{IL6}

mice were significantly enlarged, consistent with documented evidence of IL-6 induced peripheral T cell expansion[15] (**Figure 4A**). We therefore hypothesized that the extreme levels of IL-6 generated in the pancreas of OT-PDAC^{IL6} mice facilitated immune cell expansion and immune-mediated tumor clearance. We used flow cytometry to evaluate the immune profile of OT-PDAC^{IL6} and OT-PDAC^{parental} tumors and discovered that pancreata bearing OT-PDAC^{IL6} tumors were enriched with CD4^{+} T cells and Natural Killer (NK) cells, while Foxp3^{+} T-regulatory cells were decreased (**Figure 4B-I**). Because increased tumor-infiltrating lymphocytes are associated with improved outcomes and therapeutic efficacy, we next assessed the localization of T cells relative to tumor[21]. By immunofluorescent staining, we found that OT-PDAC^{parental} and OT-PDAC^{IL6} mice had equal densities of CD3^{+} T cells in both tumor-associated stroma and tumor nests (**Figure 4J-L**). These data were initially contradictory to the flow cytometry data. However, upon histological assessment, we found that OT-PDAC^{IL6} pancreata exhibited a significantly greater number of tumor-associated lymphoid aggregates (**Figure 4M-N**). In PDAC, lymphoid aggregate formation is associated with improved survival[22, 23]. In OT-PDAC^{IL6} mice, the lymphoid aggregates were often near, but not necessarily located within tumor stroma, which accounts for the differences between our flow cytometry and immunofluorescence data. In summary, locally high IL-6 induces accumulation of lymphoid aggregates, increased CD4^{+} T cells, and decreased Foxp3^{+} T regulatory cells. These conditions favor the hypothesis that tumor clearance occurs via an anti-tumor T cell response.

T cells are necessary for OT-PDAC^{IL6} tumor clearance. Based on our flow cytometry analysis, we hypothesized that T cells are necessary for OT-PDAC^{IL6} tumor clearance, which we tested using CD4 and CD8 depletion antibodies, compared to IgG control treatment. Mice

received antibody injections two days before tumor implantation and every four days following. We validated T cell depletion via flow cytometry for total T cells (CD90.2), and $CD4^+$ and $CD8^+$ cells (**Figure 5A-C**). We followed humane endpoints for the CD4/CD8-depleted group, which reached euthanasia criteria at 8-11 days post implantation (**Figure 5D**). We euthanized all sham and IgG-treated mice when all CD4/CD8-depleted mice were euthanized, although they were healthy at the time. We used a second engineered cell line, $PDAC^{IL6\text{-}LUC}$, which expressed luciferase, to measure tumor burden over time. Both OT-$PDAC^{IL6\text{-}LUC}$ longitudinal data, and OT-$PDAC^{IL6}$ endpoint tumor mass data show that CD4/CD8-depletion prevents tumor clearance (**Figure 5E-G**). Histological evaluation by a board-certified pathologist found tumor present in 10/10 CD4/CD8-depleted mice, and in 1/8 IgG control mice (**Figure 5H**). This was supported by *Il6*-transgene qPCR data and plasma IL-6 levels, which showed no elevation of IL-6 in 6/8 IgG-treated PDAC mice (**Figure 5I-J**). We conclude that CD4 and CD8 T cells are necessary for OT-$PDAC^{IL6}$ tumor clearance.

Because we previously saw recovery of wasting phenotypes in OT-$PDAC^{IL6}$ mice as the tumor resolved, we also investigated cachexia resolution in T cell-depleted mice. CD4/CD8 depletion prevented body mass recovery and led to sustained muscle wasting as evidenced by decreased muscle mass and increased atrophy-related gene expression (*Trim63, Fbxo32*) (**Figure 5K-M**). The recovery in wasting is therefore directly associated with immune-mediated tumor clearance.

OT-$PDAC^{IL6}$ induces a durable T cell response to OT-$PDAC^{Parental}$ tumors. Given the dependency of the anti-OT-$PDAC^{IL6}$ response on T cells, which are known to elicit immunologic memory, we hypothesized that OT-$PDAC^{IL6}$ tumors would generate a durable

immune response that would protect mice in the case of a second tumor exposure. We first tested this hypothesis in a cohort of mice that had recovered from sham surgery or OT-PDAC^{IL6} for over two months, and rechallenged mice with OT-PDAC$^{parental\text{-}LUC}$ (luciferase-expressing) at 76 days after initial surgery (**Figure 6A**). Sham-recovered mice implanted with PDAC$^{parental\text{-}LUC}$ reached euthanasia criteria 13-14 days post rechallenge implantation. There were no deaths during rechallenge in the OT-PDAC^{IL6}-recovered group (**Figure 6B**). Tumor burden measured longitudinally by IVIS and terminally (in sham-recovered mice only) revealed significant tumor growth only in sham-recovered mice (**Figure 6C-D**). Sham-recovered mice also lost more body mass than OT-PDAC^{IL6}-recovered mice during rechallenge (**Figure 6E**). These data indicate that the potent anti-tumor immune response elicited by high concentrations of IL-6 is durable and not dependent on coincident supraphysiologic IL-6 levels. We then used CD4/CD8 antibody depletion to determine whether the tumor clearance during rechallenge was indeed T cell-mediated. In this study, all mice recovered from OT-PDAC^{IL6} for 26 days before starting antibody treatment and were given sham surgery or implanted with OT-PDAC^{parental} tumors on day 28. We monitored mice for 12 days, until CD4/CD8-depleted mice reached humane euthanasia criteria (**Figure 6F**). We confirmed that clearance of the rechallenge OT-PDAC^{parental} tumor is dependent on T cells, which were effectively depleted by the antibody treatment (**Figure 6G-I**). Furthermore, we confirmed that CD4/CD8-depletion does not result in outgrowth of potentially covert PDAC^{IL6} cells, as there was no tumor present in the OT-PDAC^{IL6}-recovered, sham-rechallenged, CD4/CD8-depleted mice (**Figure 6G**). These data show that the T cell response induced by OT-PDAC^{IL6} provides durable protection against molecularly similar PDAC tumor growth.

DISCUSSION

Our model of PDAC IL-6 overexpression induces a robust, rapid, and durable anti-tumor T cell response that is accompanied by rapid and severe wasting, which recovers as the tumor is cleared. Although IL-6 is traditionally viewed as a negative actor in pancreatic cancer [8-11], we provide evidence that supraphysiologic levels of IL-6 are sufficient to induce an anti-tumor immune landscape in the pancreas characterized by: increased lymphoid aggregate formation, elevated $CD4^+$ T cells, and decreased $Foxp3^+$ Treg cells. While the KxPxCx tumor line implanted orthotopically exhibited complete, recurrence-free survival, subcutaneous tumors of the same line displayed less complete and slower regression in tumor size. IL-6 overexpression in other KPC cell lines (1199 and 1242) resulted in significant improvements in mouse survival time, although tumors were never fully cleared and mice did progress to humane euthanasia endpoints. These cases highlight that the magnitude of anti-tumor immunity due to IL-6 overexpression is partially dependent cell-line intrinsic properties.

Unlike cancer types that are now successfully treated with immunotherapy, survival rates for PDAC patients have increased very slowly over the past decade[24]. PDAC is highly immunosuppressive, causing immunotherapies, such as checkpoint blockade, to be ineffective clinically [25]. Previous work indicates that enhancing T cell activation using exogenous agents, such as agonistic anti-CD40 antibody, improves response to checkpoint blockade therapies and PDAC tumor regression[1]. Our work provides a basis for pursuing IL-6 as an alternative method to improve T cell response.

Our work raises a fundamental contradiction regarding the role of IL-6 in PDAC. We propose that the effect of IL-6 on PDAC growth is pleiotropic and concentration-dependent. At low concentrations, IL-6 aids tumor development via signaling directly on neoplastic cells to drive

transformation and growth. At supraphysiologic concentrations seen in OT-PDAC^{IL6} tumor-bearing mice, IL-6 stimulates an anti-tumor immune response. Circulating levels are approximately 100 times higher than what we detect in OT-PDAC^{parental} mice, and we presume that local concentrations in the pancreas are even higher. We can infer that tumor-derived IL-6 is the initiating signal for T cell accumulation and eventual tumor clearance, however, the precise manner in which IL-6 mediates this remains unknown. In addition to increased numbers of tumor-infiltrating T cells, we detected increased NK cells, increased neutrophils, and decreased Treg cells intratumorally. It is possible that IL-6, which is a known immunomodulatory cytokine, impacts multiple cell populations simultaneously to orchestrate an anti-tumor immune microenvironment[26].

Our data support the widely-accepted notion that IL-6 induces acutely negative effects, as evidenced by rapid body mass loss of 10-15% in OT-PDAC^{IL6} mice (**Figure 2H**). From a reductionist perspective, this model will open doors to understanding IL-6-mediated T cell activation in PDAC and the intricacies of cachexia resolution after PDAC tumor clearance. Future work will focus on identifying the immune subpopulations that integrate IL-6 signaling into a T cell response, with the goal of identifying targetable drivers of the anti-tumor response. This will be clinically meaningful as leaning on high-dose IL-6, a known driver of cachexia, is likely dangerous for already vulnerable patients with PDAC.

ACKNOWLEDGEMENTS

We thank all members of the Aaron Grossberg, Robert Eil, and Katelyn Byrne labs for their helpful discussion and suggestions. We also acknowledge the expert technical assistance by

staff in the Advanced Multiscale Microscopy Shared Resource and Histopathology Shared Resource. Author contributions are: Conceptualization, PCAW, AQB, RE, AJG. Methodology, PCAW, AQB, KTB, RE, AJG. Validation, PCAW, AQB, HM, XZ, JD, MM, PRL, PD. Formal Analysis, PCAW, AQB, HM, XZ, JD, PD, GDS, AJG. Investigation, PCAW, AQB, HM, XZ, JD, MM, PRL, PD, GDS. Writing—Original Draft, PCAW. Writing – Review and Editing, PCAW, AQB, KTB, RE, AJG. Visualization, PCAW, AQB, PD. Supervision, RE, AJG. Project Administration, RE, AJG. Funding Acquisition, PCAW, RE, AJG. All authors approved this manuscript.

METHODS

Mouse Studies

Husbandry

C57BL/6J (WT, JAX 000664) mice were purchased from The Jackson Laboratory (Bar Harbor, ME) and maintained in our animal facility. All mice were housed and bred in a dedicated mouse room maintained at 26 °C, 40% humidity, and 12-h light/dark cycle. Mice were provided *ad libitum* access to food and water (5L0D, PicoLab) unless otherwise stated. All mice were 12 weeks of age at experiment start. Sex in each experiment is defined in the figure legends. When single housed, mice were allowed a 7-day acclimation period prior to procedure/study start. All tumor studies followed humane endpoints. All mice were humanely euthanized via cardiac puncture or cervical dislocation under deep isoflurane anesthesia. Mouse studies were conducted in accordance with the NIH Guide for the Care and Use of Laboratory animals, and approved by the Oregon Health & Science University IACUC.

Orthotopic Tumor Implantation

A vial of frozen KPC cells was thawed prior to each implantation, and 1 million cells were implanted in 23 uL of PBS per mouse. All mice were anesthetized with isoflurane, scrubbed with betadine, and a para-midline incision was made in the abdomen to expose pancreas. KPC cells or vehicle (PBS) were injected directly into the pancreatic parenchyma. Pancreas was placed back into position and incision was closed using two sutures (4-0 Polysorb) and two skin staples.

Subcutaneous Tumor Implantation

A vial of frozen KPC cells was thawed prior to each implantation, and 1 or 2 million cells were implanted in 100 uL of PBS per mouse. The mouse's lower right abdomen was shaved, then the needle was inserted near the right 4th mammary gland.

IVIS imaging

Mice were injected with 100 uL of 15 mg/mL D-luciferin potassium salt in DPBS (no Ca, no Mg) (GoldBio, #LUCK-100), then anesthetized with isoflurane. 10 minutes later, a luminescent image and photo were captured. Longitudinal data was analyzed in one batch by normalizing tumor ROI luminescence total counts to average background ROI luminescence total counts.

Antibody-based depletion

Mice were dosed intraperitoneally (IP) with either a combination of CD4 (BioXcell, #BE0003-1) and CD8a (BioXcell, #BE0061) depletion antibodies, or Rat IgG2b isotype control antibody

(BioXcell, #BE0090), which were resuspended in InVivoPure ph7.0 Dilution Buffer (BioXcell, #IP0070) per the manufacturer's instructions. First dose was 0.2 mg each antibody per mouse, given IP two days prior to tumor implantation. Following doses were 0.1 mg each antibody per mouse, given IP every 4 days after initial dose.

Cell lines

Growth Conditions and validation

All cells were maintained at 37°C and 5% CO_2 in a humidified incubator, and tested negative in house for mycoplasma using Universal Mycoplasma Detection Kit (30-1012K). *Kras*$^{G12D/+}$, *Tp53*$^{R172H/+,}$ *Pdx1-Cre* (KPC) cell lines was generously shared by Dr. Elizabeth Jaffee (KxPxCx) and Dr. David Tuveson (1199 and 1242)[18-20, 27]. KPC cells were grown on tissue culture-treated dishes in growth media consisting of RPMI (Gibco) with 10% FBS (Corning) and 1% penicillin/streptomycin (Gibco).

Engineered KPC

KPC cells expressing the surface marker Thy1.1 (CD90.1) with blasticidin resistance (BSR), IL-6 with puromycin resistance, and luciferase with hygromycin resistance, were generated from our stock of KPC cells (female) described above. IL-6 sequence was codon-optimized for efficient expression (**Figure S4**). Platinum-E ecotropic packaging cells were transfected with plasmid DNA encoding MSGV-Thy1.1, MSGV-IL6-Puro, or MSGV-Luciferase as described previously[28]. Retroviral supernatants were spiked with 2ug/mL polybrene and were mixed 1:1 with fresh media before adding to 6-well tissue culture treated plates. Cells were spun at 2000g for 90min, 32C, no brake. Cells were then incubated at 37C for 48 hours before

washing off the viral supernatant and adding DMEM media (Gibco) supplemented with 10% FBS (Corning). Two days later, KPC cells were placed in complete DMEM media containing puromycin (5ug/mL) and/or blasticidin (5ug/mL) and/or hygromycin (500 ug/mL) to select for transduced cells. Following antibiotic selection, successful transduction was confirmed via flow cytometry staining for Thy1.1. KPC-CD90.1, KPC^{IL6}, and KPC^{LUC} cells were implanted for OT-PDAC as described for parental KPC cells. Continued culturing of engineered cells was done in selection media described.

Flow cytometry

Brefeldin A injections: For intracellular cytokine staining for flow cytometry, we followed previously published protocols for golgi transport blockade[29]. Briefly, each mouse received 100ug Brefeldin A (Selleckchem) injected retro-orbitally 5 hours prior to tissue collection.

Sample preparation

We collected tumors from mice 5 days post implantation, and tumors were weighed, then placed in PBS on ice. Tumor tissue was minced and digested (7). After dissociation, we strained tumor suspension through at 100 um filter, and performed ACK lysis. We collected spleens from mice at the endpoint specified. Spleens were pressed through a 70 um filter, rinsed with PBS, pelleted at 1500 RPM for 5 minutes, and lysed with ACK lysis.

Staining

We stained samples with live/dead stain (1:2000) and surface protein antibodies (1:200 each), and incubated for 20 minutes room temperature (**Table S3**). After staining, we washed samples with FACS buffer and pelleted. For intracellular staining (Foxp3), we fixed and

permeabilized cells with 4% paraformaldehyde (BD Cytofix/Cytoperm), washed cells, and then resuspended cells in antibody diluted 1:200 in permeabilization buffer (BD Perm/Wash) with overnight incubation at 4C . The next day we washed and resuspended cells with FACS buffer prior to analysis.

Instrumentation and analysis

All samples were analyzed in the OHSU Flow Cytometry Shared Resource using the Cytek Aurora flow cytometer (Cytek Biosystems), data was analyzed in FlowJoTM v10.8.1. Samples were first gated according to size and single cells, then all live cells were captured. The live population was gated on CD45+ cells to capture all leukocytes. To identify T cells, leukocytes were gated on CD90.2 then sub-gated for CD4+ or CD8+ cells. The CD4+ T cell population was gated on Foxp3 to assess T regulatory cells. Natural killer (NK) cells were sub-gated from the parental CD45+ gate. All NK1.1+ cells were captured, and then divided by expression of CD90.2 to classify as NK (conventional, CD90.2-) or NK T cells (CD90.2+).

Histology

Pancreas/tumor tissue was fixed overnight in 4% PFA, then stored in 70% ethanol. Tissues were paraffin embedded, sectioned, and hematoxylin and eosin (H&E) stained by the OHSU Histopathology Shared Resource. Tumor tissue was sectioned in 5um slices at levels 50 um apart. H&E stained tumor cross-sections were evaluated by a board-certified gastrointestinal pathologist. All samples were blinded during sectioning/staining and during evaluation. 3-5 depths of tissue were qualitatively assessed per mouse. For day 5 tumor samples, 2 depths of tissue were quantified per mouse and averaged together. For day 12 tumor samples, 1 section

was quantified.

Immunofluorescent staining and quantification

Pancreas/tumor tissue was dissected, transferred to BD Cytofix/Cytoperm diluted to 1% PFA, and kept at 4C overnight. Tissue was then transferred to 30% sucrose in PBS and kept at 4C overnight. Tissue was then washed twice in PBS before embedding in OCT media (Sakura). Tissue was cut at 8 um onto superfrost plus slides and stored at -80C until staining. To stain, slides were washed with PBS, blocked with 2.5% BSA 0.3% TritonX in PBS for one hour, stained with pre-conjugated antibodies (**Table S3**) for 1h, washed with PBS, quenched with TrueView Autofluorescence Quench kit (Vector, SP-8400) 2-5 min, stained with DAPI diluted 1:1000 for 10 min, and mounted with Vectashield Vibrance mounting medium (Vector, H-1700). Whole tissue sections were imaged on a Zeiss Axio Scan 7 at 20x magnification. Two tissue sections at least 344 um apart were assessed per sample. All images were blinded prior to annotation and analysis. In QuPath (V0.5.1), areas of tumor, as defined as PanCK positive, and stroma, as defined as PanCK negative abnormal tissue, were annotated. Adjacent tissue sections were stained with H&E and used as reference for areas of stroma. Annotations were made using only the DAPI and PanCK stains. After annotation, $CD3^+$ cells ($CD3^+$, $DAPI^+$, PanCK-) were manually counted in stroma and tumor areas. Final counts were normalized to total area of stroma or tumor annotation.

Plasma analytes

Plasma was collected, snap frozen in liquid nitrogen, and stored at -80ºC. Plasma concentrations of IL-6 (Biolegend) were measured using ELISA, and read on a plate reader

(BioTek).

Quantitative real-time polymerase chain reaction (qPCR)

We isolated RNA from cell pellets or tissue samples using the E.Z.N.A. Total RNA Kit I (Omega BioTek) and we prepared cDNA using high-capacity cDNA reverse transcription kit (Applied Biosystems). qPCR was run on the ABI 7300 (Applied Biosystems), using TaqMan Fast Advanced PCR master mix (Applied Biosystems) or SYBR Green master mix (Applied Biosystems). Relative expression was calculated using the $\Delta\Delta C_t$ method. To confirm the presence/absence of *Il6 transgene* in tumor-implanted mice, we performed 30 cycles of qPCR on the ABI7300, followed by running the PCR product on a 3% ethidium bromide gel to determine the presence of a band at the expected size of 131 bp. Primers/probes are listed in **Table S2**.

Statistical Analysis

Specific statistical tests and sample size for each study is indicated in the figure legends. Error bars in figures show SEM. Statistical analyses were performed using GraphPad Prism (version 9; GraphPad Software Inc) or JMP Pro (version 16; SAS Institute Inc), and graphs were built using GraphPad Prism (GraphPad Software Inc) statistical analysis software. P values are 2 sided with values less than 0.05 regarded as statistically significant.

Data Availability

All authors had access to the study data and had reviewed and approved the final manuscript.

All data will be available on the public repository, Mendeley Data, upon publication. Further information and resources, including plasmid sequences, engineered KPC cells, and raw data will be shared upon reasonable request to Aaron J. Grossberg (grossber@ohsu.edu).

FIGURES AND FIGURE LEGENDS

Figure 1

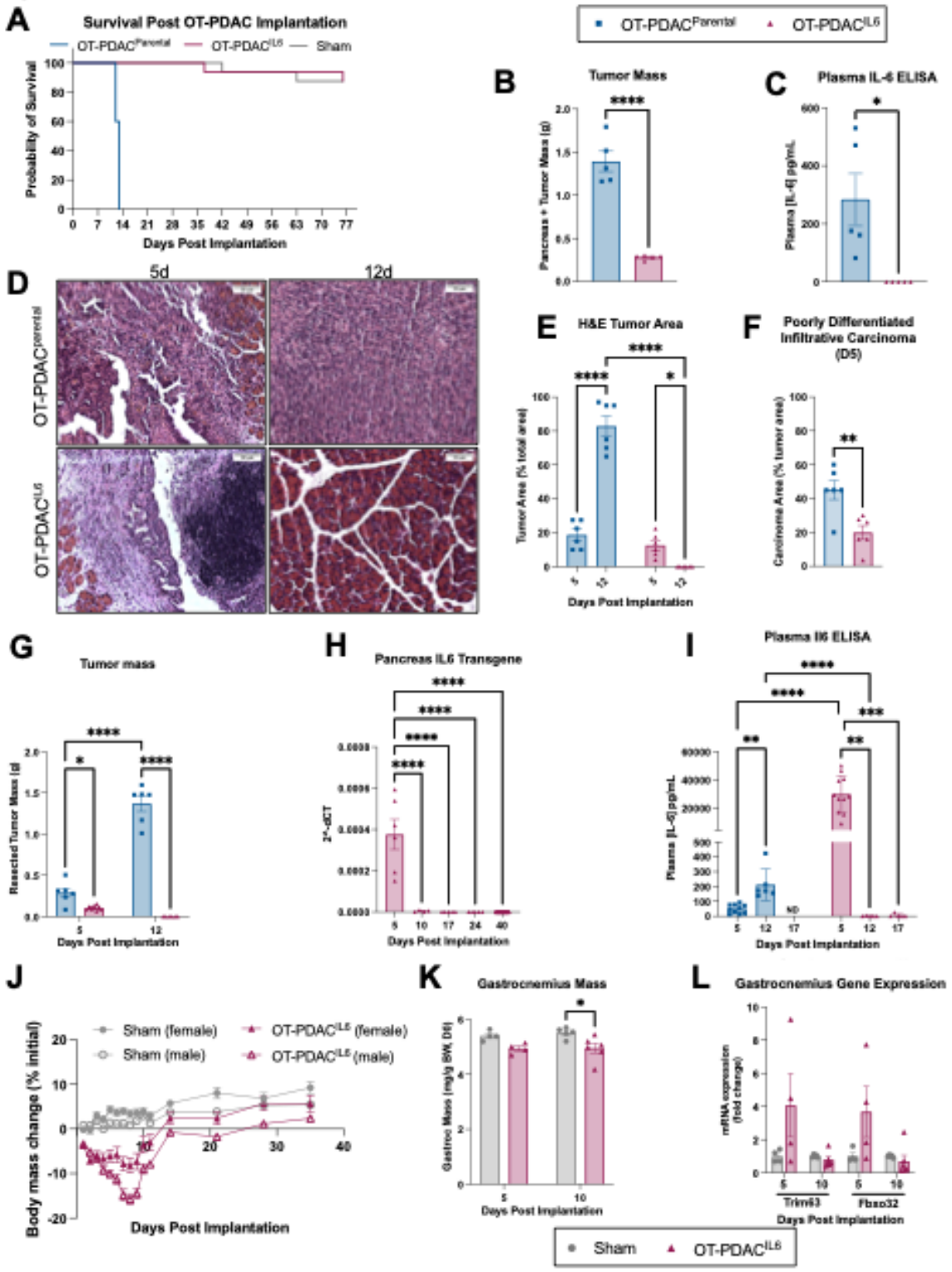

Figure 1: OT-PDAC^{IL6} results in complete tumor clearance and body mass recovery. (A) Survival comparison of OT-PDAC^{Parental} and OT-PDAC^{IL6}. N = 8 female, 8 male Sham and PDAC^{IL6}, 1 female, 4 male PDAC^{parental} mice. Statistically tested with Log-rank (Mantel-Cox) test. (B) Tumor mass at humane endpoint (OT-PDAC^{Parental}). Pancreas mass of OT-PDAC^{IL6} euthanized at a pre-determined endpoint of 24 days (did not meet humane euthanasia criteria); tumor tissue was not present. Statistically tested with 2-way ANOVA main effects only with Tukey correction for multiple comparisons. (C) Plasma IL-6 levels at the endpoints indicated in (H), Il-6 was below the assay detection limit for OT-PDAC^{IL6} mice. Statistically tested with 2-way ANOVA main effects only with Tukey correction for multiple comparisons. (A-C) N = 2 female, 3 male PDAC^{IL6}, 1 female, 4 male PDAC^{parental} mice. (D) Representative pancreas cross sections at 5 (left) and 10 days (right) from OT-PDAC^{parental} (top) and OT-PDAC^{IL6} (bottom) tumor implantation. Scale bars represent 50 um (top) and 100 um (bottom). (E) Tumor area as a percent of total tissue area at 5 and 12 days, quantified by board-certified pathologist. (F) Percentage of tumor area classified as poorly-differentiated, infiltrative carcinoma at 5 days by board-certified pathologist. (G) Tumor mass at 5 and 12 days. (B-D) N = 3 male, 3 female mice per group. (H) Expression of *Il6 transgene* expression, measured by qPCR at 5 (N = 3 male, 3 female), 10 (N = 6 male), 17 (N = 3 male, 2 female), 24 (N = 3 male, 2 female), and 40 (N = 16 male, 16 female) days. Statistically tested with One-way ANOVA with Tukey correction for multiple comparisons. (I) Plasma IL-6 measured by ELISA at 5 (N = 10 male PDAC^{Parental}, 11 male PDAC^{IL6}), 12(N = 3 male, 3 female PDAC^{Parental}, 3 male, 2 female PDAC^{IL6}), and 17 (N = 2 male, 3 female PDAC^{IL6}) days. Statistically tested with 2-way ANOVA main effects only with Tukey correction for multiple comparisons. (J) Body mass change as a percentage of initial body mass over time. N = 8 male, 8 female mice per group.

Statistically tested with 3-way ANOVA. $p<0.0001$ for Time, Sex, Tumor Status, Time x Sex, Time x Tumor Status. $p=0.0002$ for Sex x Tumor Status. $p= 0.2900$ for Time x Sex x Tumor Status. (K) Gastrocnemius muscle mass normalized to initial body mass. (L) Atrophy-related gene expression (*Trim63* and *Fbxo32*) in gastrocnemius muscle, measured by qPCR. (J-L) 5d N = 1 female, 3 male mice per group. 10d N = 6 male PDAC, 5 male sham mice. Error bars represent SEM. Unless otherwise noted, 2x2 studies were statistically tested with a full effects model 2-way ANOVA and Sidak multiple comparisons test. 2-group analysis tested with unpaired t-test. **** $p<0.0001$, ***$p<0.001$, **$p<0.01$, *$p<0.05$.

Figure 2

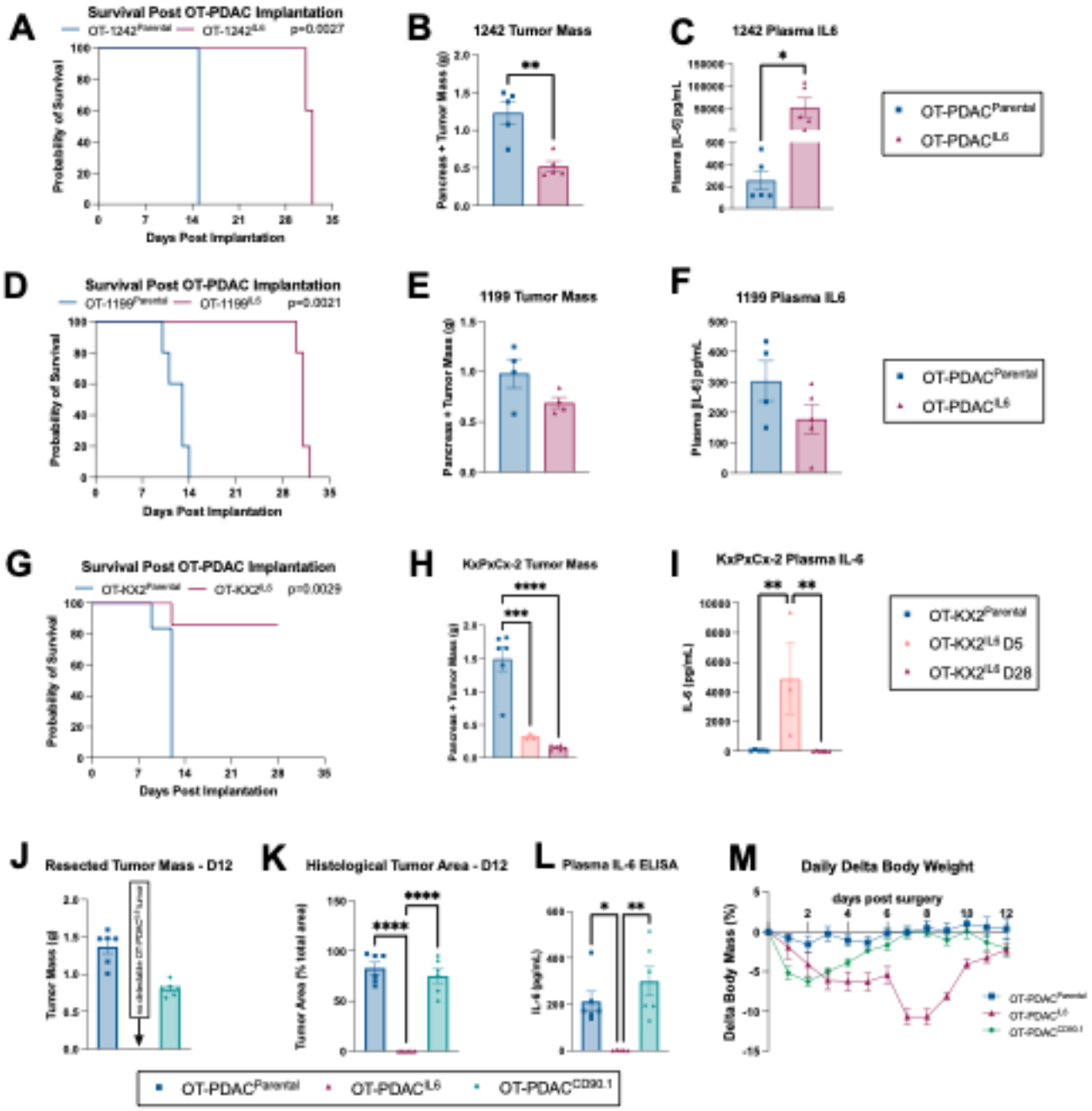
A
Survival Post OT-PDAC Implantation
OT-1242Parental
OT-1242IL6
p=0.0027
Probability of Survival
Days Post Implantation
B
1242 Tumor Mass
Pancreas + Tumor Mass (g)
C
1242 Plasma IL6
Plasma [IL-6] pg/mL
OT-PDACParental
OT-PDACIL6
D
Survival Post OT-PDAC Implantation
OT-1199Parental
OT-1199IL6
p=0.0021
Probability of Survival
Days Post Implantation
E
1199 Tumor Mass
Pancreas + Tumor Mass (g)
F
1199 Plasma IL6
Plasma [IL-6] pg/mL
OT-PDACParental
OT-PDACIL6
G
Survival Post OT-PDAC Implantation
OT-KX2Parental
OT-KX2IL6
p=0.0029
Probability of Survival
Days Post Implantation
H
KxPxCx-2 Tumor Mass
Pancreas + Tumor Mass (g)
I
KxPxCx-2 Plasma IL-6
IL-6 (pg/mL)
OT-KX2Parental
OT-KX2IL6 D5
OT-KX2IL6 D28
J
Resected Tumor Mass - D12
Tumor Mass (g)
K
Histological Tumor Area - D12
Tumor Area (% total area)
L
Plasma IL-6 ELISA
IL-6 (pg/mL)
M
Daily Delta Body Weight
days post surgery
Delta Body Mass (%)
OT-PDACParental
OT-PDACIL6
OT-PDACCD90.1

467

Figure 2: Tumor-cell IL-6 overexpression transduction controls. A) Survival comparison of Sham, OT-1242^{Parental} and OT-1242^{IL6}. Statistically tested with Log-rank (Mantel-Cox) test on pairwise comparisons. (B) Pancreas and tumor mass at humane endpoint. (C) Plasma IL-6 levels at humane endpoint. (D) Survival comparison of Sham, OT-1199 ^{Parental} and OT-1199^{IL6}. Statistically tested with Log-rank (Mantel-Cox) test on pairwise comparisons. (E) Pancreas and tumor mass at humane endpoint. (F) Plasma IL-6 levels at humane endpoint. (A-F) N= 5 male mice per group. (G) Survival comparison of Sham, OT-KX2^{Parental} and OT-KX2^{IL6}. Statistically tested with Log-rank (Mantel-Cox) test on pairwise comparisons. (H) Pancreas and tumor mass at humane endpoint (OT-KX2^{Parental}); 5 and 28 days (OT-KX2^{IL6}). Statistically tested with one-way ANOVA. (I) Plasma IL-6 levels at humane endpoint. (G-I) N = 3 male mice OT-KX2^{IL6} d5, 6 male mice OT-KX2^{IL6} d28 and OT-KX2^{parental}. (J-M) Control-transduced PDAC cells (OT-PDAC$^{CD90.1}$) do not spontaneously clear. (J) Tumor mass at 12 days post implantation. (K) Tumor area as a percent of total tissue area at 12 days post implantation, quantified by board-certified pathologist. (L) Plasma IL-6 measured by ELISA at 12 days post implantation. (M) Body mass change as a percentage of initial body mass over time. Statistically tested with one-way ANOVA analysis with repeated measures. $p<0.0001$ for Time and Time x Tumor Status. $p=0.0002$ for Tumor Status. (J-M) N = 3 male, 3 female mice per group. Error bars represent SEM. Unless otherwise noted, 2-group studies were statistically tested with unpaired t-test. 3-group studies were statistically tested with 1-way ANOVA and Sidak multiple comparisons test. **** $p<0.0001$, ***$p<0.001$, **$p<0.01$, *$p<0.05$.

Figure 3

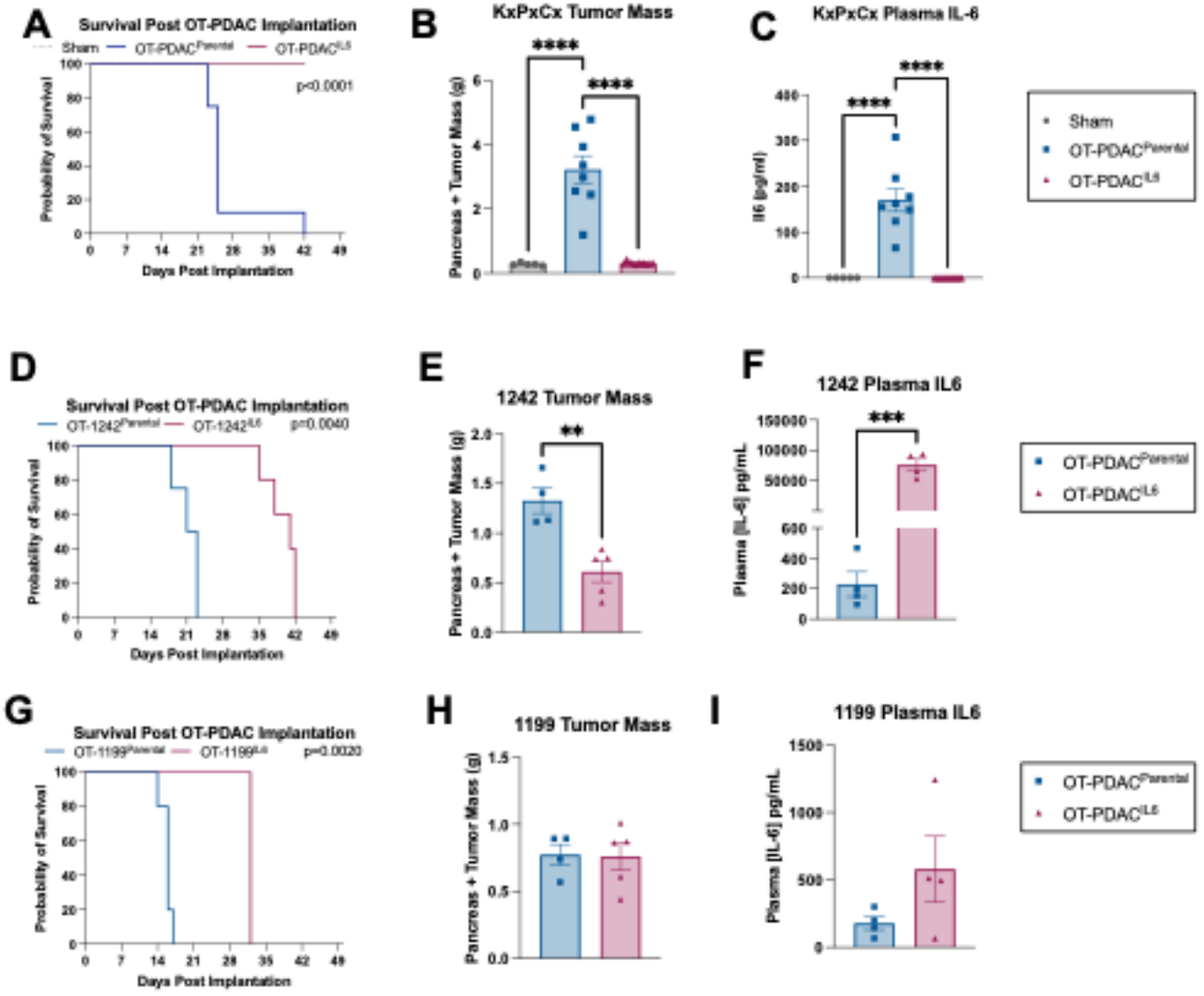
A
Survival Post OT-PDAC Implantation
Sham
OT-PDAC Parental
OT-PDAC IL6
p<0.0001
Probability of Survival
Days Post Implantation
B
KxPxCx Tumor Mass
****
****
Pancreas + Tumor Mass (g)
C
KxPxCx Plasma IL-6
****
****
Il6 (pg/ml)
Sham
OT-PDAC Parental
OT-PDAC IL6
D
Survival Post OT-PDAC Implantation
OT-1242 Parental
OT-1242 IL6
p=0.0040
Probability of Survival
Days Post Implantation
E
1242 Tumor Mass
**
Pancreas + Tumor Mass (g)
F
1242 Plasma IL6
***
Plasma [IL-6] pg/mL
OT-PDAC Parental
OT-PDAC IL6
G
Survival Post OT-PDAC Implantation
OT-1199 Parental
OT-1199 IL6
p=0.0020
Probability of Survival
Days Post Implantation
H
1199 Tumor Mass
Pancreas + Tumor Mass (g)
I
1199 Plasma IL6
Plasma [IL-6] pg/mL
OT-PDAC Parental
OT-PDAC IL6

Figure 3: Effects of tumor-specific IL-6 overexpression are maintained with lower tumor inoculation. (A) Survival comparison of OT-KxPxCx^{Parental} and OT-KxPxCx^{IL6} mice implanted with 5,000 cells. Statistically tested with Log-rank (Mantel-Cox) test on pairwise comparisons. (B) Pancreas and tumor mass at humane endpoint (OT-KxPxCx^{Parental}); 42 days (OT-KxPxCx^{IL6}). (C) Plasma IL-6 levels at endpoint. (A-C) N = 11 male mice (OT-KxPxCx^{IL6}), 8 male mice (OT-KxPxCx^{Parental}), and 5 male mice (sham). (D) Survival comparison of Sham, OT-1242^{Parental} and OT-1242^{IL6}. Statistically tested with Log-rank (Mantel-Cox) test on pairwise comparisons. (E) Pancreas and tumor mass at humane endpoint. (F) Plasma IL-6 levels at humane endpoint. (G) Survival comparison of Sham, OT-1199 ^{Parental} and OT-1199^{IL6}. Statistically tested with Log-rank (Mantel-Cox) test on pairwise comparisons. (H) Pancreas and tumor mass at humane endpoint. (I) Plasma IL-6 levels at humane endpoint. Error bars represent SEM. Unless otherwise noted, 2-group studies were statistically tested with unpaired t-test. 3-group studies were statistically tested with 1-way ANOVA and Sidak multiple comparisons test. **** $p<0.0001$, ***$p<0.001$, **$p<0.01$, *$p<0.05$.

Figure 4

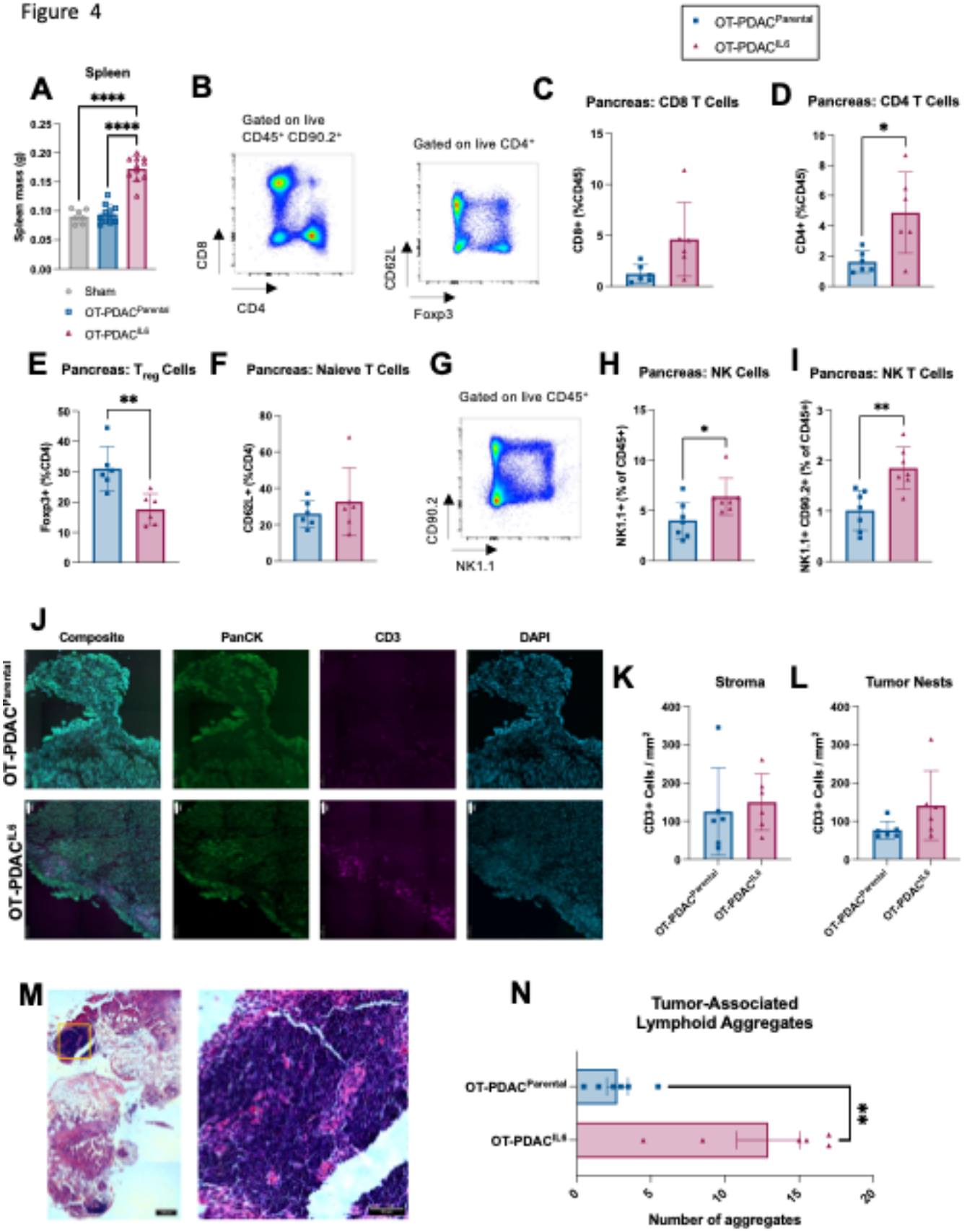
OT-PDAC^Parental
OT-PDAC^IL6
A
Spleen
Spleen mass (g)
Sham
B
Gated on live CD45+ CD90.2+
CD8
CD4
Gated on live CD4+
CD62L
Foxp3
C
Pancreas: CD8 T Cells
CD8+ (%CD45)
D
Pancreas: CD4 T Cells
CD4+ (%CD45)
E
Pancreas: Treg Cells
Foxp3+ (%CD4)
F
Pancreas: Naieve T Cells
CD62L+ (%CD4)
G
Gated on live CD45+
CD90.2
NK1.1
H
Pancreas: NK Cells
NK1.1+ (% of CD45+)
I
Pancreas: NK T Cells
NK1.1+ CD90.2+ (% of CD45+)
J
Composite
PanCK
CD3
DAPI
OT-PDAC^Parental
OT-PDAC^IL6
K
Stroma
CD3+ Cells / mm²
L
Tumor Nests
M
N
Tumor-Associated Lymphoid Aggregates
Number of aggregates

508

Figure 4: OT-PDAC^{IL6} induces lymphocytic anti-tumor immune response. (A) Spleen mass at 5 days. N = 6 male mice per group. (B-I) Intra-tumoral immune cell populations from pancreas at 5 days: (B) Representative flow gating strategy for T cells. (C) CD8^{+} T cells, (D) CD4^{+} T cells, (E) Foxp3^{+} T regulatory cells, (F) CD62L^{+} Naive T cells. (G) Representative flow gating strategy for NK cells. (H) NK1.1^{+} Natural Killer cells, (I) NK1.1^{+}/CD90.2^{+} NK T cells. (B-F) N = 6 male mice per group. (G-I) N = 4 female, 3 male mice per group. (J) representative images of CD3^{+} T cell infiltration in tumor and associated stroma of OT-PDAC^{parental} (top) and OT-PDAC^{IL6} (bottom) mice. Tissues were stained with DAPI (blue), CD3 (magenta), and Pancytokeratin (PanCK, green). (scale bars = 100 um). (K-L) CD3^{+} cells counted per mm^{2} of stroma (K) or tumor nests (L) in immunofluorescence stained pancreas tissues. N = 3 male, 3 female mice per group. (M) Representative H&E image of lymphoid aggregates adjacent to tumor and stroma in OT-PDAC^{IL6} pancreas (left) and magnified image of lymphoid aggregate (right). Area of magnification is denoted on left image with orange box. (N) Pathologist-evaluated number of tumor-associated lymphoid aggregates in H&E stained pancreas cross sections from tissue collected at 5 days. N = 3 male, 3 female mice per group. Error bars represent SEM. 2-group analysis tested with unpaired t-test. **** $p<0.0001$, ***$p<0.001$, **$p<0.01$, *$p<0.05$.

Figure 5

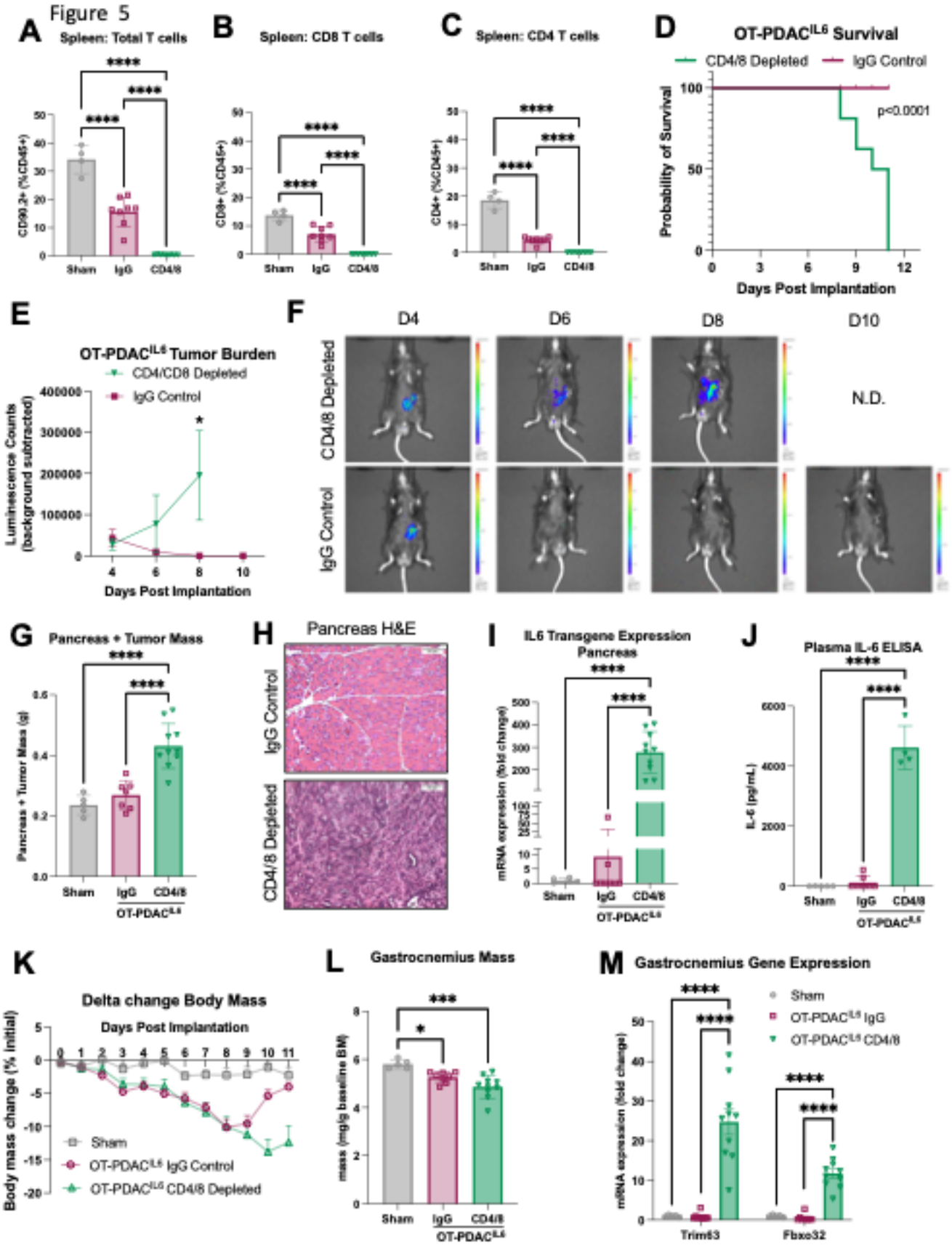
A
Spleen: Total T cells
CD90.2+ (%CD45+)
Sham
IgG
CD4/8
B
Spleen: CD8 T cells
CD8+ (%CD45+)
C
Spleen: CD4 T cells
CD4+ (%CD45+)
D
OT-PDAC^IL6 Survival
CD4/8 Depleted
IgG Control
p<0.0001
Probability of Survival
Days Post Implantation
E
OT-PDAC^IL6 Tumor Burden
CD4/CD8 Depleted
IgG Control
Luminescence Counts (background subtracted)
Days Post Implantation
F
D4
D6
D8
D10
CD4/8 Depleted
IgG Control
N.D.
G
Pancreas + Tumor Mass
Pancreas + Tumor Mass (g)
OT-PDAC^IL6
H
Pancreas H&E
IgG Control
CD4/8 Depleted
I
IL6 Transgene Expression Pancreas
mRNA expression (fold change)
J
Plasma IL-6 ELISA
IL-6 (pg/mL)
K
Delta change Body Mass
Days Post Implantation
Body mass change (% initial)
Sham
OT-PDAC^IL6 IgG Control
OT-PDAC^IL6 CD4/8 Depleted
L
Gastrocnemius Mass
mass (mg/g baseline BM)
M
Gastrocnemius Gene Expression
mRNA expression (fold change)
Sham
OT-PDAC^IL6 IgG
OT-PDAC^IL6 CD4/8
Trim63
Fbxo32

527

Figure 5: CD4^{+} and CD8^{+} T cells are necessary for OT-PDAC^{IL6} tumor clearance. (A-C) Confirmation of CD4/CD8a T cell depletion via flow cytometry on spleen 12 days post implantation for (A)CD90.2+ total T cells, (B) CD8+ T cells, (C) CD4+ T cells. (D) Survival comparison of OT-PDAC^{IL6} mice given CD4/CD8 depletion or IgG control antibodies. Statistically tested with Log-rank (Mantel-Cox) test. (E) OT-PDAC$^{IL6\text{-}LUC}$ tumor growth, measured by IVIS imaging. Statistically tested with 2-way ANOVA, for time points with representation from both groups, with Šídák multiple testing correction. (F) Representative images from IVIS imaging of OT-PDAC$^{IL6\text{-}LUC}$ 10 minutes after luciferin injection. Images are of the same animals longitudinally. CD4/CD8 depleted mice reached humane endpoint prior to D10 scan. (G) Pancreas and tumor mass at endpoint. (H) Representative pancreas cross sections at humane euthanasia endpoint from IgG control (top) and CD4/CD8 depleted (bottom) mice. Scale bars represent 100 um. (I) expression of *Il6 transgene* expression, measured by qPCR. (J) Plasma IL-6 measured by ELISA. (K) Body mass change as a percentage of initial body mass over time. Statistically tested with Mixed-effects analysis with repeated measures. $p<0.0001$ for Time and Time x Tumor Status. $p=0.0048$ for Tumor Status. (L) Gastrocnemius muscle mass at humane euthanasia endpoint normalized to initial body mass. (M) Atrophy-related gene expression (*Trim63* and *Fbxo32*) in gastrocnemius muscle, measured by qPCR. All male mice, N = 5 sham, 10 PDAC^{IL6} per antibody treatment group. Error bars represent SEM. 3 group studies were statistically tested with a 1-way ANOVA and Tukey correction for multiple comparisons. **** $p<0.0001$, ***$p<0.001$, **$p<0.01$, *$p<0.05$.

Figure 6

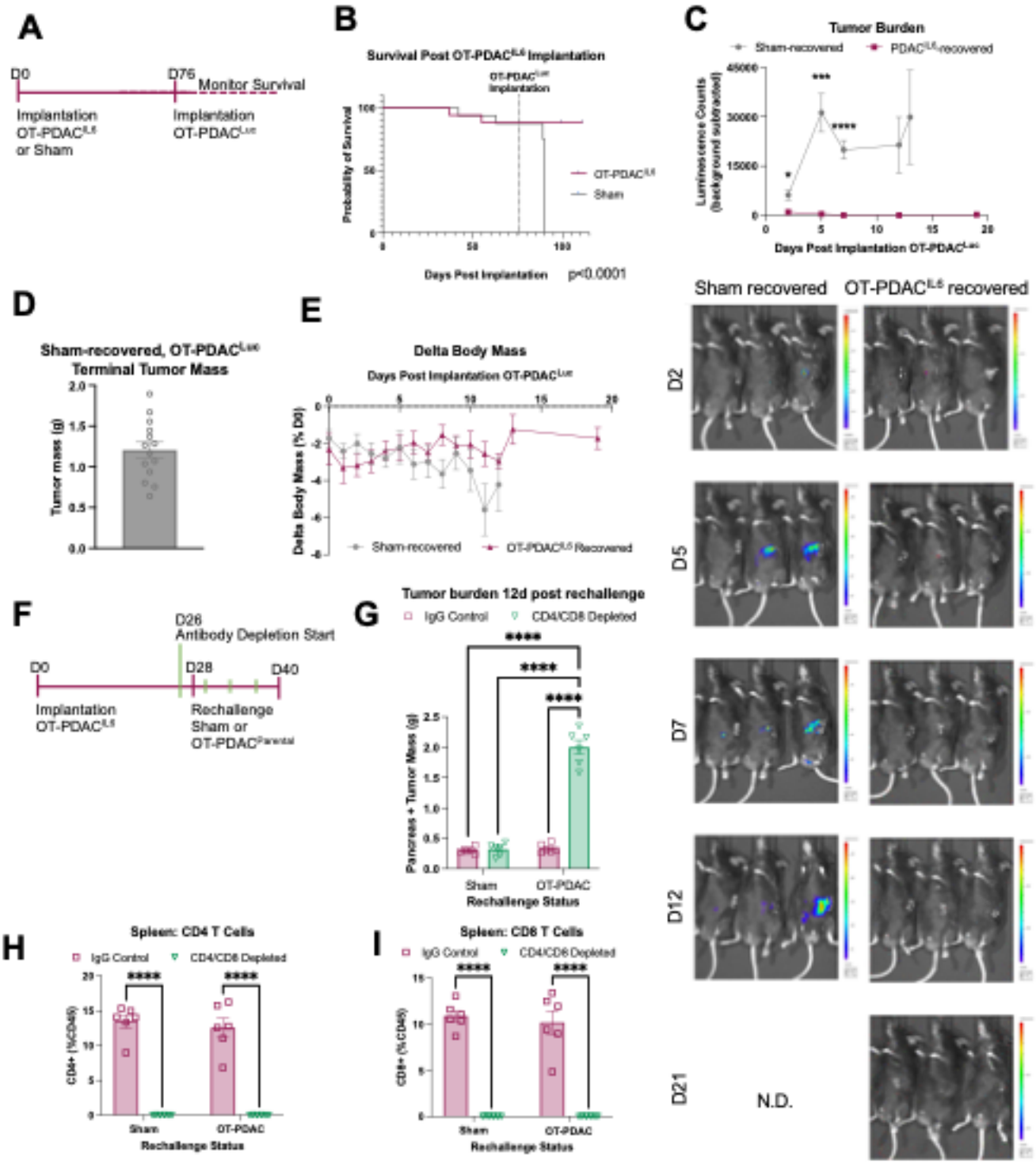
A
D0
D76
Monitor Survival
Implantation OT-PDAC^{IL6} or Sham
Implantation OT-PDAC^{Luc}
B
Survival Post OT-PDAC^{IL6} Implantation
OT-PDAC^{Luc} Implantation
Probability of Survival
OT-PDAC^{IL6}
Sham
Days Post Implantation
p<0.0001
C
Tumor Burden
Sham-recovered
PDAC^{IL6}-recovered
Luminescence Counts (background subtracted)
Days Post Implantation OT-PDAC^{Luc}
D
Sham-recovered, OT-PDAC^{Luc} Terminal Tumor Mass
Tumor mass (g)
E
Delta Body Mass
Days Post Implantation OT-PDAC^{Luc}
Delta Body Mass (% D0)
Sham-recovered
OT-PDAC^{IL6} Recovered
Sham recovered
OT-PDAC^{IL6} recovered
D2
D5
D7
D12
D21
N.D.
F
D26 Antibody Depletion Start
D0
D28
D40
Implantation OT-PDAC^{IL6}
Rechallenge Sham or OT-PDAC^{Parental}
G
Tumor burden 12d post rechallenge
IgG Control
CD4/CD8 Depleted
Pancreas + Tumor Mass (g)
Sham
OT-PDAC
Rechallenge Status
H
Spleen: CD4 T Cells
IgG Control
CD4/CD8 Depleted
CD4+ (%CD45)
Sham
OT-PDAC
Rechallenge Status
I
Spleen: CD8 T Cells
IgG Control
CD4/CD8 Depleted
CD8+ (%CD45)
Sham
OT-PDAC
Rechallenge Status

549

Figure 6: OT-PDAC^{IL6} induces a durable T cell response to OT-PDAC^{Parental} tumors. (A) Schematic timeline for B-E. Mice were implanted with OT-PDAC^{IL6} or given sham surgery, then all mice were rechallenged with OT-PDAC$^{Parental\text{-}LUC}$ after 76 days. (B) Survival comparison of OT-PDAC^{IL6}-recovered and sham-recovered mice. Statistically tested with Log-rank (Mantel-Cox) test. (C) OT-PDAC$^{Parental\text{-}LUC}$ tumor growth, measured by IVIS imaging. Statistically tested with mixed effects model and Šídák multiple testing correction, using imputation to match PDAC^{IL6} endpoint with the sham endpoint. Corresponding IVIS images below. (D) Tumor mass at humane euthanasia endpoint for sham-recovered OT-PDAC$^{Parental\text{-}LUC}$ tumors. (E) Body mass change as a percentage of initial body mass over time. Statistically tested with mixed effects model and Šídák multiple testing correction at timepoints where both groups were represented. p=0.0435 for Time, p=0.4903 for Tumor Status, p=0.0002 for Time x Tumor Status. (A-E) N = 7 male PDAC^{IL6}, 8 male sham, 7 female PDAC^{IL6}, 6 female sham. (F) Schematic timeline for G-I. Mice were implanted with OT-PDAC^{IL6} or given Sham surgery. 28 days later, mice were rechallenged with OT-PDAC^{Parental}, and given CD4/CD8 depletion or IgG control antibodies beginning on D26 and every 4 days thereafter (denoted with double green lines). (G) Pancreas/tumor mass at 12 days. (H) Intra-tumoral CD4^{+} T cells at 12 days. (I) Intra-tumoral CD8^{+} T cells at 12 days. (F-I) All male mice N = 6 per group. Error bars represent SEM. 2x2 studies were statistically tested with a full effects model 2-way ANOVA and Sidak multiple comparisons test. **** p<0.0001, ***p<0.001, **p<0.01, *p<0.05.

REFERENCES

1. Winograd R, Byrne KT, Evans RA, et al. Induction of T-cell immunity overcomes complete resistance to PD-1 and CTLA-4 blockade and improves survival in pancreatic carcinoma. Cancer immunology research 2015;3:399-411.
2. Beatty GL, Eghbali S, Kim R. Deploying immunotherapy in pancreatic cancer: defining mechanisms of response and resistance. American Society of Clinical Oncology Educational Book 2017;37:267-278.
3. Aznar MA, Good CR, Barber-Rotenberg JS, et al. Clinical and molecular dissection of CAR T cell resistance in pancreatic cancer. Cell Reports Medicine 2025.
4. Byrne KT, Vonderheide RH. CD40 stimulation obviates innate sensors and drives T cell immunity in cancer. Cell reports 2016;15:2719-2732.
5. Gnerlich JL, Mitchem JB, Weir JS, et al. Induction of Th17 cells in the tumor microenvironment improves survival in a murine model of pancreatic cancer. The Journal of Immunology 2010;185:4063-4071.
6. Delvecchio FR, Fincham RE, Spear S, et al. Pancreatic cancer chemotherapy is potentiated by induction of tertiary lymphoid structures in mice. Cellular and Molecular Gastroenterology and Hepatology 2021;12:1543-1565.
7. Hotz C, Wagenaar TR, Gieseke F, et al. Local delivery of mRNA-encoded cytokines promotes antitumor immunity and tumor eradication across multiple preclinical tumor models. Science translational medicine 2021;13:eabc7804.
8. Corcoran RB, Contino G, Deshpande V, et al. STAT3 plays a critical role in KRAS-induced pancreatic tumorigenesis. Cancer research 2011;71:5020-5029.
9. Suh S-Y, Choi YS, Yeom CH, et al. Interleukin-6 but not tumour necrosis factor-alpha

predicts survival in patients with advanced cancer. Supportive Care in Cancer 2013;21:3071-3077.

10. Rupert JE, Narasimhan A, Jengelley DH, et al. Tumor-derived IL-6 and trans-signaling among tumor, fat, and muscle mediate pancreatic cancer cachexia. Journal of Experimental Medicine 2021;218:e20190450.

11. Razidlo GL, Burton KM, McNiven MA. Interleukin-6 promotes pancreatic cancer cell migration by rapidly activating the small GTPase CDC42. Journal of Biological Chemistry 2018;293:11143-11153.

12. Arneson-Wissink PC, Mendez H, Pelz K, et al. Hepatic signal transducer and activator of transcription-3 signalling drives early-stage pancreatic cancer cachexia via suppressed ketogenesis. Journal of Cachexia, Sarcopenia and Muscle 2024.

13. Flint TR, Janowitz T, Connell CM, et al. Tumor-induced IL-6 reprograms host metabolism to suppress anti-tumor immunity. Cell metabolism 2016;24:672-684.

14. Zhang Y, Yan W, Collins MA, et al. Interleukin-6 is required for pancreatic cancer progression by promoting MAPK signaling activation and oxidative stress resistance. Cancer research 2013;73:6359-6374.

15. Fujimoto M, Nakano M, Terabe F, et al. The influence of excessive IL-6 production in vivo on the development and function of Foxp3+ regulatory T cells. The Journal of Immunology 2011;186:32-40.

16. Jiang Z, Liao R, Lv J, et al. IL-6 trans-signaling promotes the expansion and anti-tumor activity of CAR T cells. Leukemia 2021;35:1380-1391.

17. Nejad EB, Labrie C, van Elsas MJ, et al. IL-6 signaling in macrophages is required for immunotherapy-driven regression of tumors. Journal for ImmunoTherapy of Cancer

2021;9:e002460.

18. Foley K, Rucki AA, Xiao Q, et al. Semaphorin 3D autocrine signaling mediates the metastatic role of annexin A2 in pancreatic cancer. Science signaling 2015;8:ra77-ra77.

19. Quaranta V, Rainer C, Nielsen SR, et al. Macrophage-derived granulin drives resistance to immune checkpoint inhibition in metastatic pancreatic cancer. Cancer research 2018;78:4253-4269.

20. Ireland L, Santos A, Ahmed MS, et al. Chemoresistance in pancreatic cancer is driven by stroma-derived insulin-like growth factors. Cancer research 2016;76:6851-6863.

21. Ino Y, Yamazaki-Itoh R, Shimada K, et al. Immune cell infiltration as an indicator of the immune microenvironment of pancreatic cancer. British journal of cancer 2013;108:914-923.

22. Hiraoka N, Ino Y, Yamazaki-Itoh R, et al. Intratumoral tertiary lymphoid organ is a favourable prognosticator in patients with pancreatic cancer. British journal of cancer 2015;112:1782-1790.

23. Sautès-Fridman C, Petitprez F, Calderaro J, et al. Tertiary lymphoid structures in the era of cancer immunotherapy. Nature Reviews Cancer 2019;19:307-325.

24. Siegel RL, Miller KD, Wagle NS, et al. Cancer statistics, 2023. CA: a cancer journal for clinicians 2023;73:17-48.

25. Hilmi M, Delaye M, Muzzolini M, et al. The immunological landscape in pancreatic ductal adenocarcinoma and overcoming resistance to immunotherapy. The Lancet Gastroenterology & Hepatology 2023.

26. Soler MF, Abaurrea A, Azcoaga P, et al. New perspectives in cancer immunotherapy: targeting IL-6 cytokine family. Journal for ImmunoTherapy of Cancer 2023;11.

27. Michaelis KA, Zhu X, Burfeind KG, et al. Establishment and characterization of a novel murine model of pancreatic cancer cachexia. Journal of cachexia, sarcopenia and muscle 2017;8:824-838.

28. Eil R, Vodnala SK, Clever D, et al. Ionic immune suppression within the tumour microenvironment limits T cell effector function. Nature 2016;537:539-543.

29. Liu F, Whitton JL. Cutting edge: re-evaluating the in vivo cytokine responses of CD8+ T cells during primary and secondary viral infections. The Journal of Immunology 2005;174:5936-5940.

Figure 1

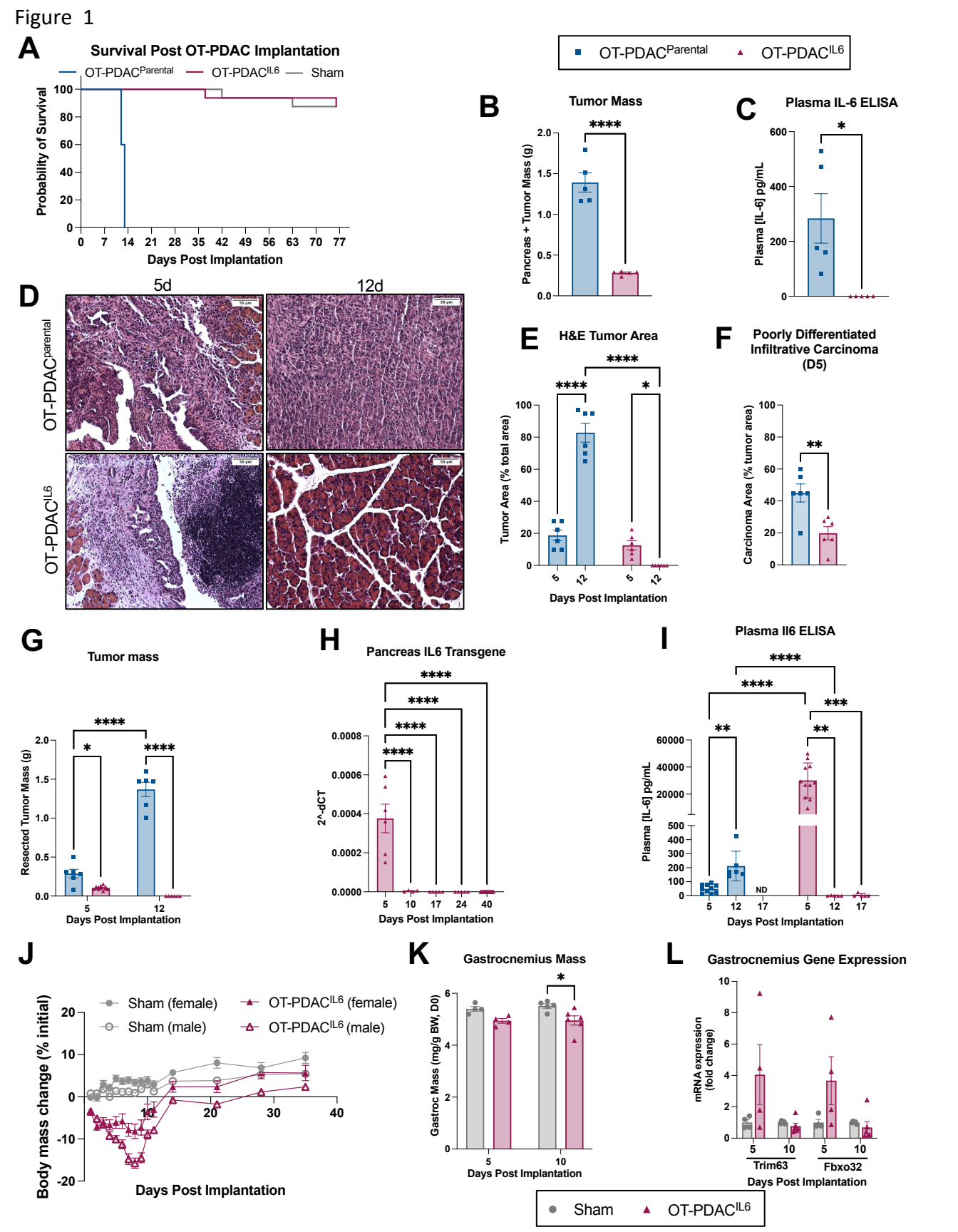
A
Survival Post OT-PDAC Implantation
OT-PDACParental
OT-PDACIL6
Sham
Probability of Survival
Days Post Implantation
OT-PDACParental
OT-PDACIL6
B
Tumor Mass
Pancreas + Tumor Mass (g)
C
Plasma IL-6 ELISA
Plasma [IL-6] pg/mL
D
5d
12d
OT-PDACparental
OT-PDACIL6
E
H&E Tumor Area
Tumor Area (% total area)
Days Post Implantation
F
Poorly Differentiated Infiltrative Carcinoma (D5)
Carcinoma Area (% tumor area)
G
Tumor mass
Resected Tumor Mass (g)
Days Post Implantation
H
Pancreas IL6 Transgene
2^-dCT
Days Post Implantation
I
Plasma Il6 ELISA
Plasma [IL-6] pg/mL
ND
Days Post Implantation
J
Sham (female)
Sham (male)
OT-PDACIL6 (female)
OT-PDACIL6 (male)
Body mass change (% initial)
Days Post Implantation
K
Gastrocnemius Mass
Gastroc Mass (mg/g BW, D0)
Days Post Implantation
L
Gastrocnemius Gene Expression
mRNA expression (fold change)
Trim63
Fbxo32
Days Post Implantation
Sham
OT-PDACIL6

Figure 2

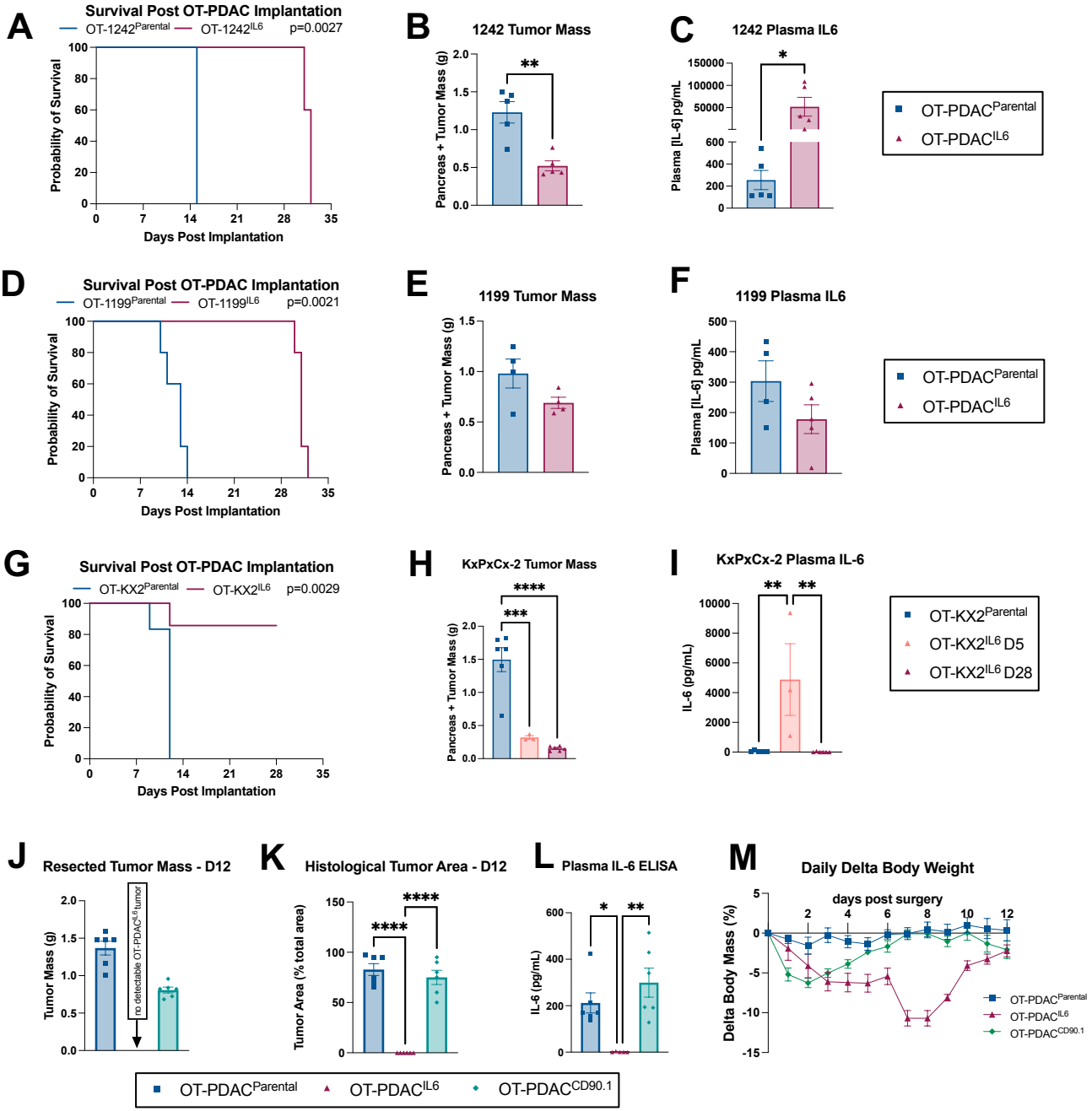
A
Survival Post OT-PDAC Implantation
OT-1242Parental
OT-1242IL6
p=0.0027
Probability of Survival
Days Post Implantation
B
1242 Tumor Mass
Pancreas + Tumor Mass (g)
**
C
1242 Plasma IL6
Plasma [IL-6] pg/mL
*
OT-PDACParental
OT-PDACIL6
D
Survival Post OT-PDAC Implantation
OT-1199Parental
OT-1199IL6
p=0.0021
Probability of Survival
Days Post Implantation
E
1199 Tumor Mass
Pancreas + Tumor Mass (g)
F
1199 Plasma IL6
Plasma [IL-6] pg/mL
OT-PDACParental
OT-PDACIL6
G
Survival Post OT-PDAC Implantation
OT-KX2Parental
OT-KX2IL6
p=0.0029
Probability of Survival
Days Post Implantation
H
KxPxCx-2 Tumor Mass
Pancreas + Tumor Mass (g)
****
***
I
KxPxCx-2 Plasma IL-6
IL-6 (pg/mL)
**
**
OT-KX2Parental
OT-KX2IL6 D5
OT-KX2IL6 D28
J
Resected Tumor Mass - D12
Tumor Mass (g)
no detectable OT-PDACIL6 tumor
K
Histological Tumor Area - D12
Tumor Area (% total area)
****
****
L
Plasma IL-6 ELISA
IL-6 (pg/mL)
*
**
M
Daily Delta Body Weight
days post surgery
Delta Body Mass (%)
OT-PDACParental
OT-PDACIL6
OT-PDACCD90.1
OT-PDACParental
OT-PDACIL6
OT-PDACCD90.1

Figure 3

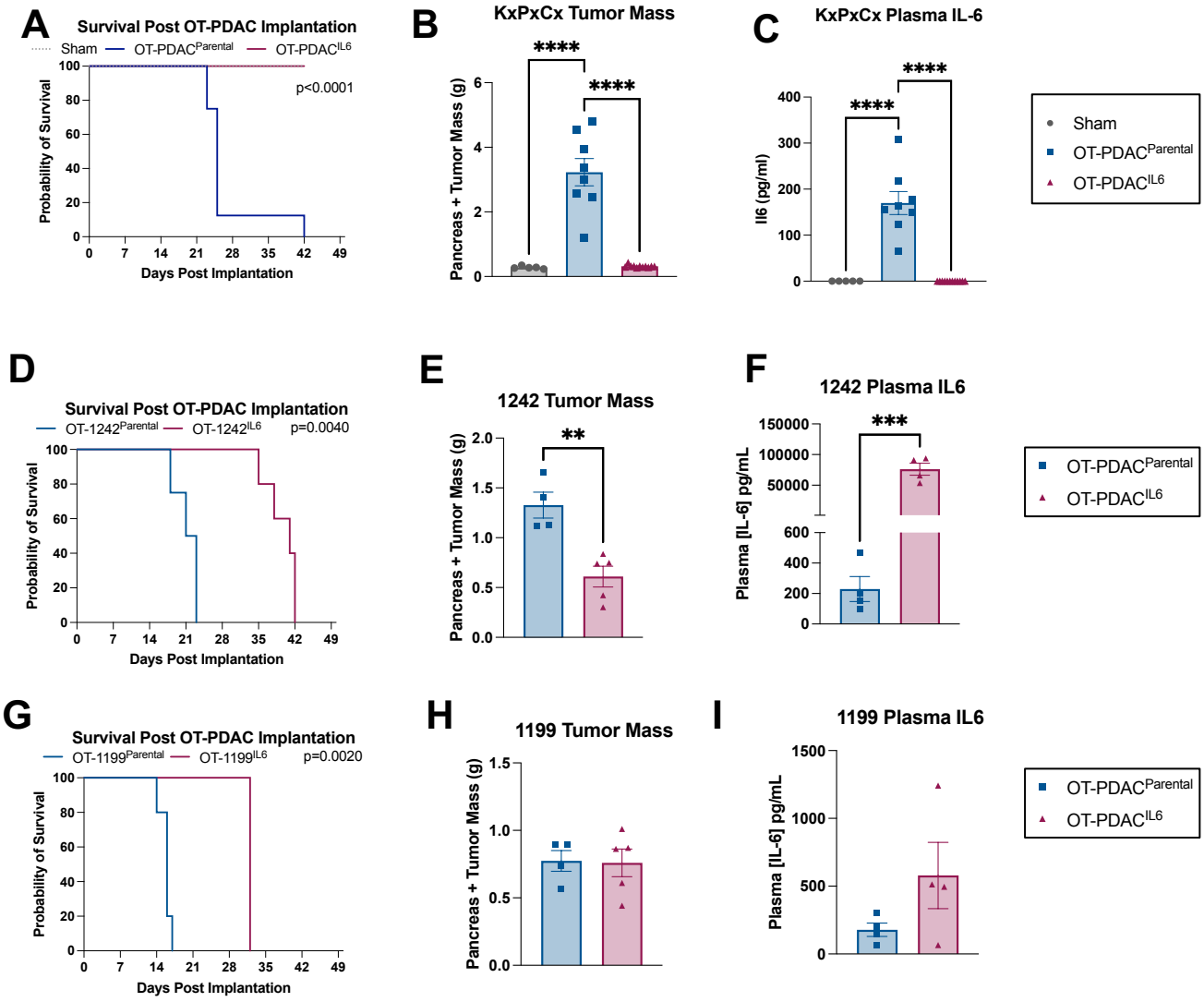
A
Survival Post OT-PDAC Implantation
Sham
OT-PDAC Parental
OT-PDAC IL6
p<0.0001
Probability of Survival
Days Post Implantation
B
KxPxCx Tumor Mass
Pancreas + Tumor Mass (g)
****
****
C
KxPxCx Plasma IL-6
Il6 (pg/ml)
****
****
Sham
OT-PDAC Parental
OT-PDAC IL6
D
Survival Post OT-PDAC Implantation
OT-1242 Parental
OT-1242 IL6
p=0.0040
Probability of Survival
Days Post Implantation
E
1242 Tumor Mass
Pancreas + Tumor Mass (g)
**
F
1242 Plasma IL6
Plasma [IL-6] pg/mL
***
OT-PDAC Parental
OT-PDAC IL6
G
Survival Post OT-PDAC Implantation
OT-1199 Parental
OT-1199 IL6
p=0.0020
Probability of Survival
Days Post Implantation
H
1199 Tumor Mass
Pancreas + Tumor Mass (g)
I
1199 Plasma IL6
Plasma [IL-6] pg/mL
OT-PDAC Parental
OT-PDAC IL6

Figure 4

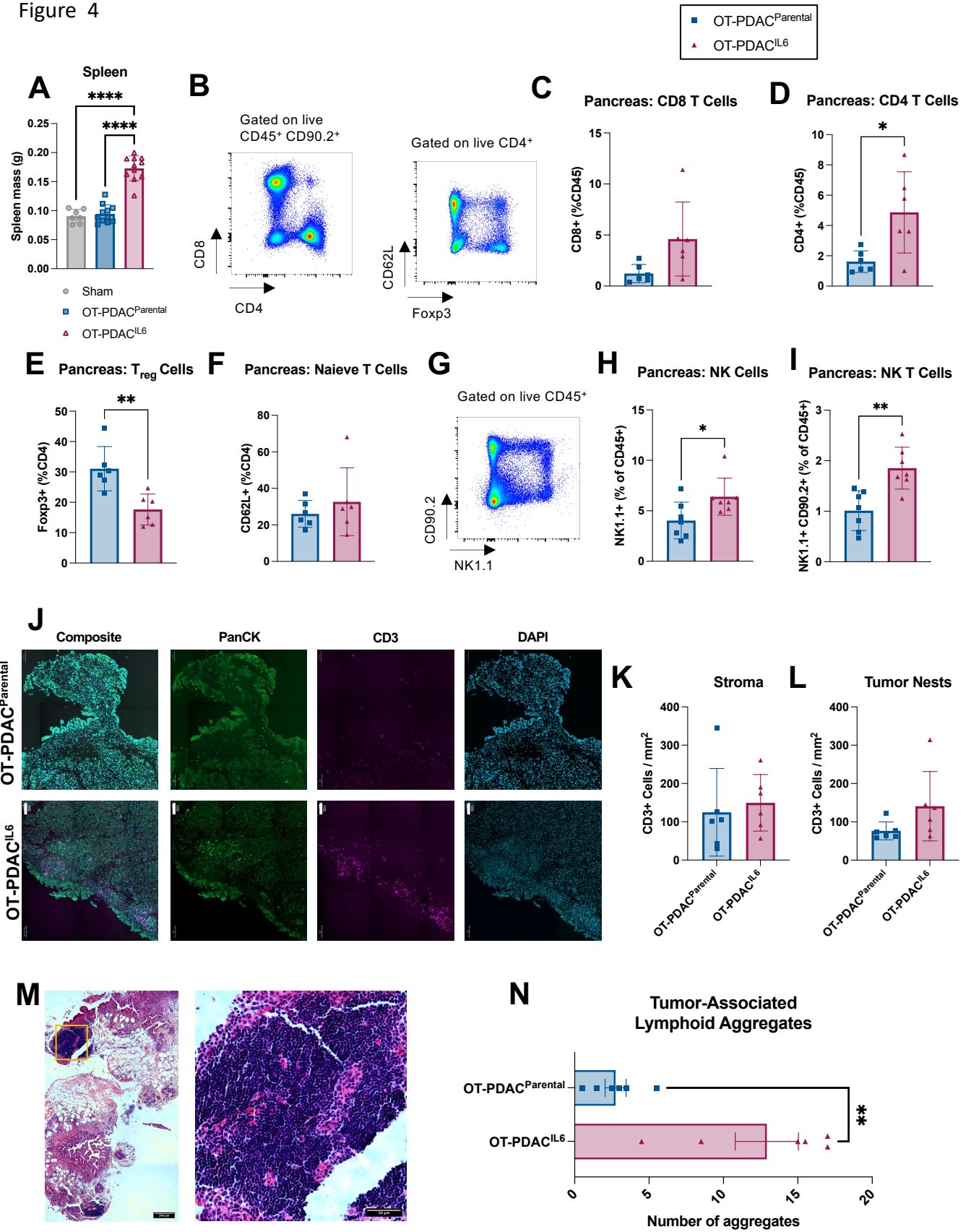
OT-PDAC^Parental
OT-PDAC^IL6
A
Spleen
****
****
Spleen mass (g)
0.25
0.20
0.15
0.10
0.05
0.00
Sham
OT-PDAC^Parental
OT-PDAC^IL6
B
Gated on live
CD45+ CD90.2+
CD8
CD4
Gated on live CD4+
CD62L
Foxp3
C
Pancreas: CD8 T Cells
CD8+ (%CD45)
D
Pancreas: CD4 T Cells
*
CD4+ (%CD45)
E
Pancreas: Treg Cells
**
Foxp3+ (%CD4)
F
Pancreas: Naieve T Cells
CD62L+ (%CD4)
G
Gated on live CD45+
CD90.2
NK1.1
H
Pancreas: NK Cells
*
NK1.1+ (% of CD45+)
I
Pancreas: NK T Cells
**
NK1.1+ CD90.2+ (% of CD45+)
J
Composite
PanCK
CD3
DAPI
OT-PDAC^Parental
OT-PDAC^IL6
K
Stroma
CD3+ Cells / mm2
L
Tumor Nests
CD3+ Cells / mm2
M
N
Tumor-Associated
Lymphoid Aggregates
OT-PDAC^Parental
OT-PDAC^IL6
**
Number of aggregates

Figure 5

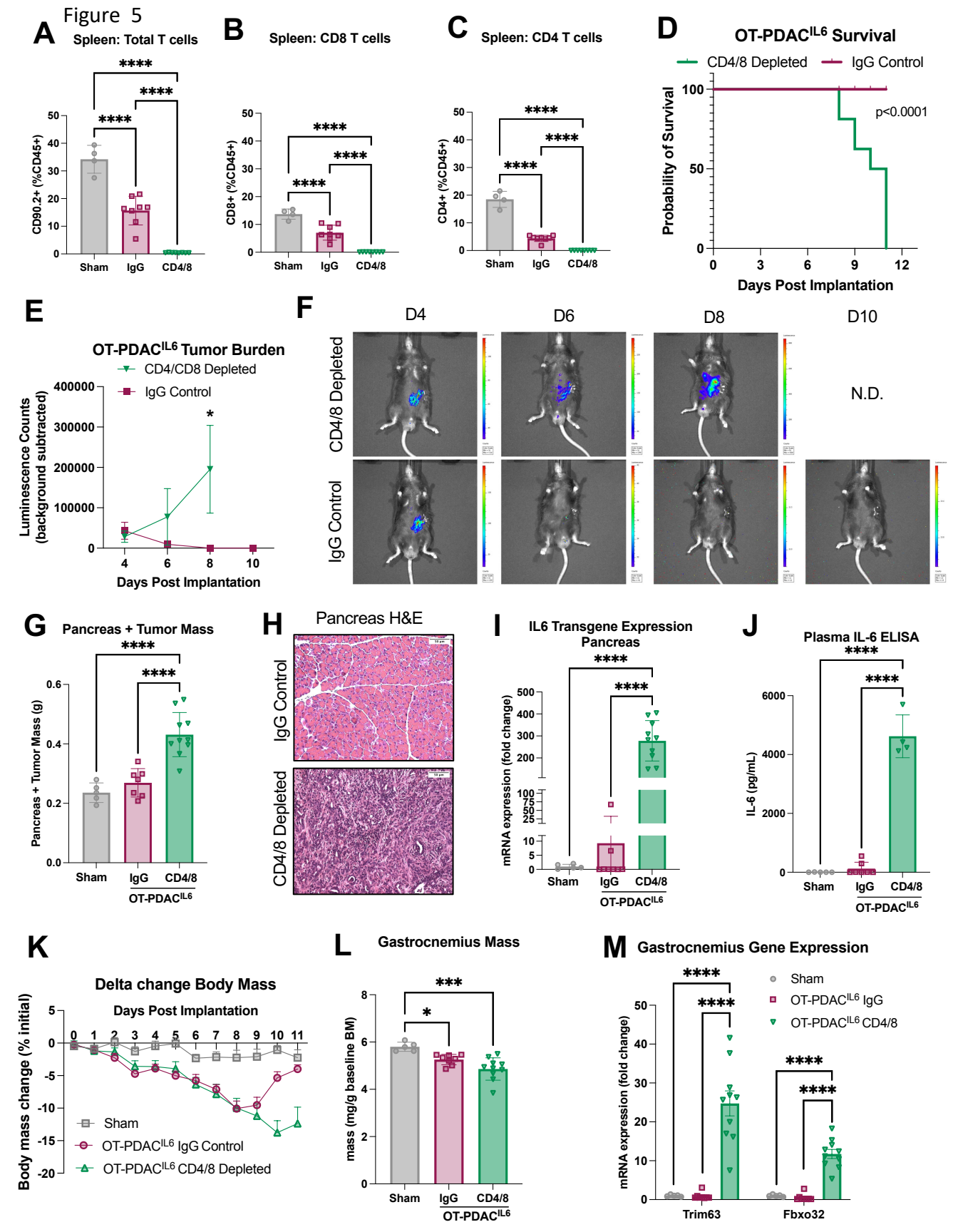
A
Spleen: Total T cells
CD90.2+ (%CD45+)
Sham
IgG
CD4/8
B
Spleen: CD8 T cells
CD8+ (%CD45+)
C
Spleen: CD4 T cells
CD4+ (%CD45+)
D
OT-PDAC^IL6 Survival
CD4/8 Depleted
IgG Control
Probability of Survival
p<0.0001
Days Post Implantation
E
OT-PDAC^IL6 Tumor Burden
CD4/CD8 Depleted
IgG Control
Luminescence Counts (background subtracted)
Days Post Implantation
F
D4
D6
D8
D10
CD4/8 Depleted
IgG Control
N.D.
G
Pancreas + Tumor Mass
Pancreas + Tumor Mass (g)
OT-PDAC^IL6
H
Pancreas H&E
IgG Control
CD4/8 Depleted
I
IL6 Transgene Expression Pancreas
mRNA expression (fold change)
OT-PDAC^IL6
J
Plasma IL-6 ELISA
IL-6 (pg/mL)
OT-PDAC^IL6
K
Delta change Body Mass
Days Post Implantation
Body mass change (% initial)
Sham
OT-PDAC^IL6 IgG Control
OT-PDAC^IL6 CD4/8 Depleted
L
Gastrocnemius Mass
mass (mg/g baseline BM)
OT-PDAC^IL6
M
Gastrocnemius Gene Expression
Sham
OT-PDAC^IL6 IgG
OT-PDAC^IL6 CD4/8
mRNA expression (fold change)
Trim63
Fbxo32

Figure 6

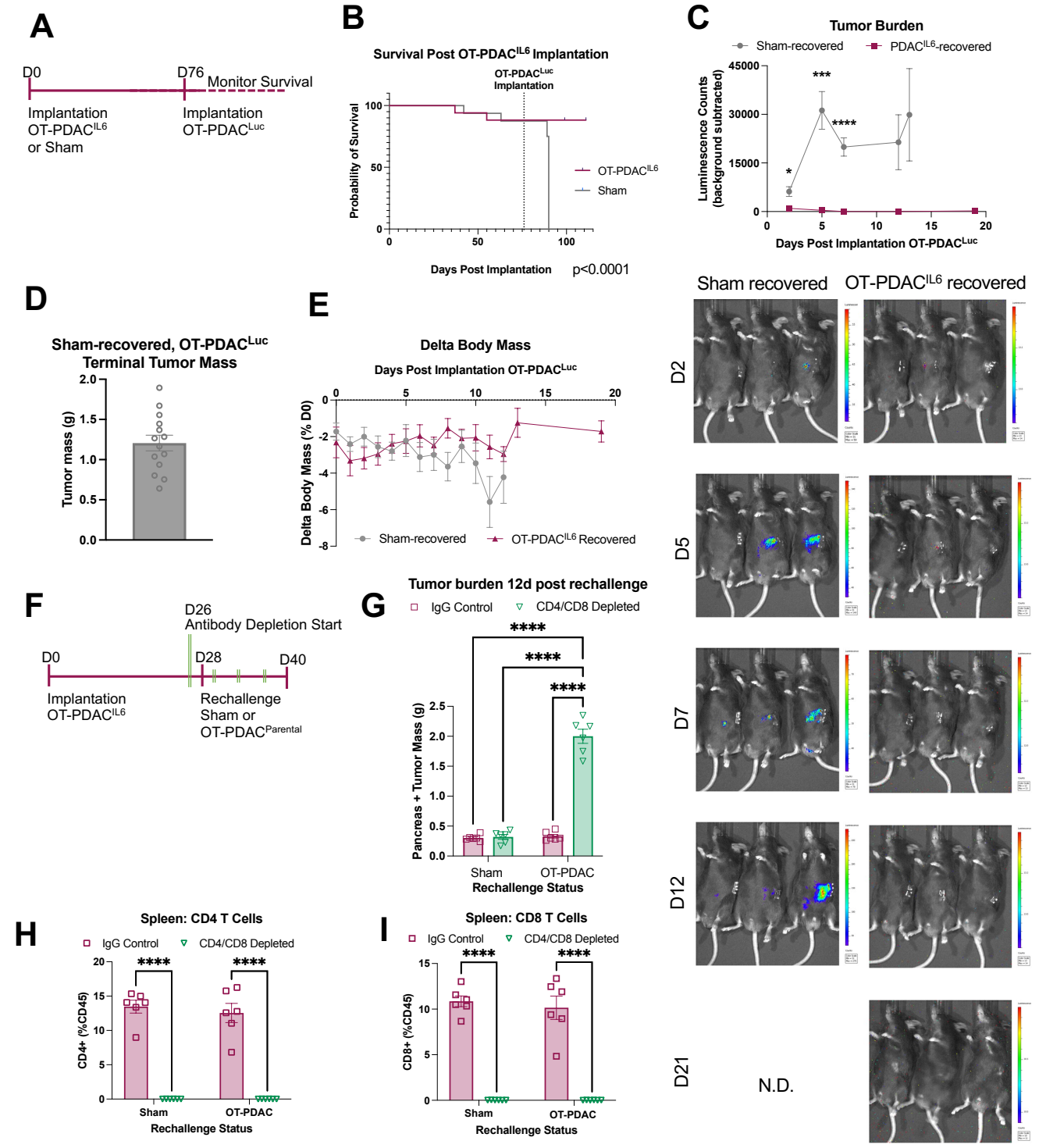
A
D0
D76
Monitor Survival
Implantation OT-PDAC^{IL6} or Sham
Implantation OT-PDAC^{Luc}
B
Survival Post OT-PDAC^{IL6} Implantation
OT-PDAC^{Luc} Implantation
Probability of Survival
OT-PDAC^{IL6}
Sham
Days Post Implantation
p<0.0001
C
Tumor Burden
Sham-recovered
PDAC^{IL6}-recovered
Luminescence Counts (background subtracted)
Days Post Implantation OT-PDAC^{Luc}
D
Sham-recovered, OT-PDAC^{Luc} Terminal Tumor Mass
Tumor mass (g)
E
Delta Body Mass
Days Post Implantation OT-PDAC^{Luc}
Delta Body Mass (% D0)
Sham-recovered
OT-PDAC^{IL6} Recovered
Sham recovered
OT-PDAC^{IL6} recovered
D2
D5
D7
D12
D21
N.D.
F
D26
Antibody Depletion Start
D0
D28
D40
Implantation OT-PDAC^{IL6}
Rechallenge Sham or OT-PDAC^{Parental}
G
Tumor burden 12d post rechallenge
IgG Control
CD4/CD8 Depleted
Pancreas + Tumor Mass (g)
Sham
OT-PDAC
Rechallenge Status
H
Spleen: CD4 T Cells
IgG Control
CD4/CD8 Depleted
CD4+ (%CD45)
Sham
OT-PDAC
Rechallenge Status
I
Spleen: CD8 T Cells
IgG Control
CD4/CD8 Depleted
CD8+ (%CD45)
Sham
OT-PDAC
Rechallenge Status